© 2020. Published by The Company of Biologists Ltd | Development (2020) 147, dev193805. doi:10.1242/dev.193805

RESEARCH ARTICLE

Harmonization of L1CAM expression facilitates axon outgrowth and guidance of a motor neuron

Tessa Sherry[1,2], Ava Handley[1], Hannah R. Nicholas[2] and Roger Pocock[1,*]

ABSTRACT

Brain development requires precise regulation of axon outgrowth, guidance and termination by multiple signaling and adhesion molecules. How the expression of these neurodevelopmental regulators is transcriptionally controlled is poorly understood. The *Caenorhabditis elegans* SMD motor neurons terminate axon outgrowth upon sexual maturity and partially retract their axons during early adulthood. Here we show that C-terminal binding protein 1 (CTBP-1), a transcriptional corepressor, is required for correct SMD axonal development. Loss of CTBP-1 causes multiple defects in SMD axon development: premature outgrowth, defective guidance, delayed termination and absence of retraction. CTBP-1 controls SMD axon guidance by repressing the expression of SAX-7, an L1 cell adhesion molecule (L1CAM). CTBP-1-regulated repression is crucial because deregulated SAX-7/L1CAM causes severely aberrant SMD axons. We found that axonal defects caused by deregulated SAX-7/L1CAM are dependent on a distinct L1CAM, called LAD-2, which itself plays a parallel role in SMD axon guidance. Our results reveal that harmonization of L1CAM expression controls the development and maturation of a single neuron.

KEY WORDS: *Caenorhabditis elegans*, L1 cell adhesion molecule, SAX-7, C-terminal binding protein, Axon guidance, Axon outgrowth

INTRODUCTION

Establishment of neuronal circuits within the brain requires choreographed events, including axon outgrowth, guidance, fasciculation and termination. Once development is complete, maintenance factors promote stable axon morphology and position throughout life (Aurelio et al., 2002; Sasakura et al., 2005), although examples of structural plasticity such as axon pruning and retraction also exist (Bagri et al., 2003; Luo and O'Leary, 2005; Xu and Henkemeyer, 2009). These complex axonal behaviors are directed by intrinsic and extrinsic molecular interactions and signaling pathways that require precise spatial and temporal control (Hutter, 2019; Tessier-Lavigne and Goodman, 1996). Ultimately, integration and harmonization of these signaling pathways enables axons to navigate complex molecular and cellular environments correctly. However, regulatory mechanisms that govern spatial and temporal control of axon guidance signals are poorly understood.

L1 cell adhesion molecules (L1CAMs) are transmembrane proteins, typically composed of six immunoglobulin (Ig) domains, three to five fibronectin III domains (FnIII) and a short cytoplasmic domain containing an ankyrin binding motif, FERM domain and PDZ domain (Brümmendorf et al., 1998). L1CAMs coordinate multiple adhesion and signaling events in nervous system development, maintenance and function (Brümmendorf et al., 1998; Cohen et al., 1998). As a result, mutations in L1 family members result in a wide range of human neurological abnormalities, including CRASH disorder (corpus callosum hypoplasia, retardation, adducted thumbs, spastic paraplegia and hydrocephalus) (Nagaraj et al., 2014). Vertebrates typically encode four L1 family members (L1, CHL1, neurofascin and NrCAM), whereas invertebrates contain one or two L1 orthologs (Brümmendorf et al., 1998). The nematode *Caenorhabditis elegans* encodes two L1CAM orthologs, LAD-2 and SAX-7, which play multiple autonomous and nonautonomous functions in axodendritic development and maintenance (Bénard et al., 2012; Chen et al., 2019, 2001; Dong et al., 2013; Pocock et al., 2008; Ramirez-Suarez et al., 2019; Salzberg et al., 2013; Sasakura et al., 2005; Wang et al., 2008). However, the regulatory mechanisms governing L1CAM expression remain largely elusive.

The SMDDs are a bilaterally symmetric pair of cholinergic motor neurons that extend axons to pioneer the *C. elegans* neuropil (nerve ring) during embryogenesis (Rapti et al., 2017). During post-embryonic development, the SMDDs extend posteriorly directed axons from the head into the dorsal sublateral nerve cord where they terminate in the anterior half of the animal. The SMDDs innervate dorsal muscles to drive head bending and regulation of omega turn amplitude, and are functionally important for exploratory behavior and proprioception (Cook et al., 2019; Gray et al., 2005; Shen et al., 2016; White et al., 1986; Yeon et al., 2018). Here, we show that C-terminal binding protein 1 (CTBP-1) controls SMDD development by regulating SAX-7/L1CAM expression. We provide genetic and molecular evidence that CTBP-1 repression of *sax-7* is required for SMDD guidance but not outgrowth. We further show that the regulatory relationship between CTBP-1 and SAX-7 controls SMDD development in a temporally distinct and parallel pathway to the other *C. elegans* L1CAM ortholog, LAD-2. Thus, appropriate expression of two L1CAMs is important for control of SMDD development, and CTBP-1-dependent transcriptional repression of SAX-7 permits the axon-promoting function of LAD-2. In vertebrates, CtBP proteins are highly expressed in the brain, and loss of CtBP2 in mice causes delayed development in the forebrain and midbrain (Hildebrand and Soriano, 2002). In humans, mutations of CtBP have been detected in patients with intellectual disability, and the ability of CtBP to act as a corepressor is crucial for correct neuronal development (Beck et al., 2016, 2019; Sommerville et al., 2017). Taken together, our results uncover a mechanism that controls axonal development by harmonizing L1CAM expression, a mechanism that might be used in vertebrates to control brain development.

[1]Development and Stem Cells Program, Monash Biomedicine Discovery Institute and Department of Anatomy and Developmental Biology, Monash University, Melbourne, Victoria 3800, Australia. [2]School of Life and Environmental Sciences, The University of Sydney, Sydney, NSW 2006, Australia.

*Author for correspondence (roger.pocock@monash.edu)

H.R.N., 0000-0002-2239-9249; R.P., 0000-0002-5515-3608

Handling Editor: François Guillemot
Received 9 June 2020; Accepted 18 September 2020

Development (2020) 147, dev193805. doi:10.1242/dev.193805

RESULTS

SMDD neurons undergo phases of axon outgrowth and retraction

The SMDDs are a pair of cholinergic sublateral motor neurons that extend dorsally directed axons to pioneer the *C. elegans* nerve ring during embryogenesis (Rapti et al., 2017). We surveyed post-embryonic development of the SMDD neurons using a *Pglr-1::GFP* transgene and found that SMDD axon outgrowth is continuous throughout larval development and the first day of adulthood, although it is not scaled with the increase in worm body length (Fig. 1A-C; Fig. S1A, Table S1). We found that termination of SMDD axon outgrowth occurs ∼170 µm from the terminal bulb of the pharynx in 1-day-old adults (Fig. 1C; Table S1). Subsequently, we observed that during days 1-3 of adulthood, the SMDD axons retract by 14 µm (∼8% of their length), with no further retraction from days 3-5 (Fig. 1C, and Table S1). We detected no associated decrease in body length during these adult stages (Fig. S1A, Table S1). These observations suggest that the SMDDs undergo autonomous axonal remodeling during postembryonic development and adulthood.

CTBP-1a controls SMDD axon outgrowth and retraction

We previously reported that the transcriptional corepressor CTBP-1 is important for SMDD axonal morphology (Reid et al., 2015). Loss of *ctbp-1* causes aberrant SMDD axon guidance, where axons turn away (curl) from the dorsal sublateral nerve cord (Fig. 1D,E) (Reid et al., 2015). We examined whether CTBP-1 also controls SMDD axon termination and/or retraction. We found that SMDD axons are longer in *ctbp-1(tm5512)* mutant animals than in the wild type at all developmental stages from L3 larvae onwards (Fig. 1F,G; Tables S1, S2). We further show that, unlike the wild type, SMDD axons of *ctbp-1(tm5512)* mutants continue to extend between days 1 and 3 of adulthood and maintain their length in day 5 adults [249 µm for *ctbp-1(tm5512)* mutants versus 158 µm for wild type; Fig. 1F; Table S2]. These data reveal that in *ctbp-1(tm5512)* mutant animals, the SMDD axons fail to terminate in early adulthood and do not retract as the worms age. Increased SMDD axonal length was independent of overall body length, as *ctbp-1* mutants were either shorter (L2-L4, D3) or had similar body length as wild-type animals (D1 and D5) (Fig. S1A, Tables S1, S2). Furthermore, the SMDD

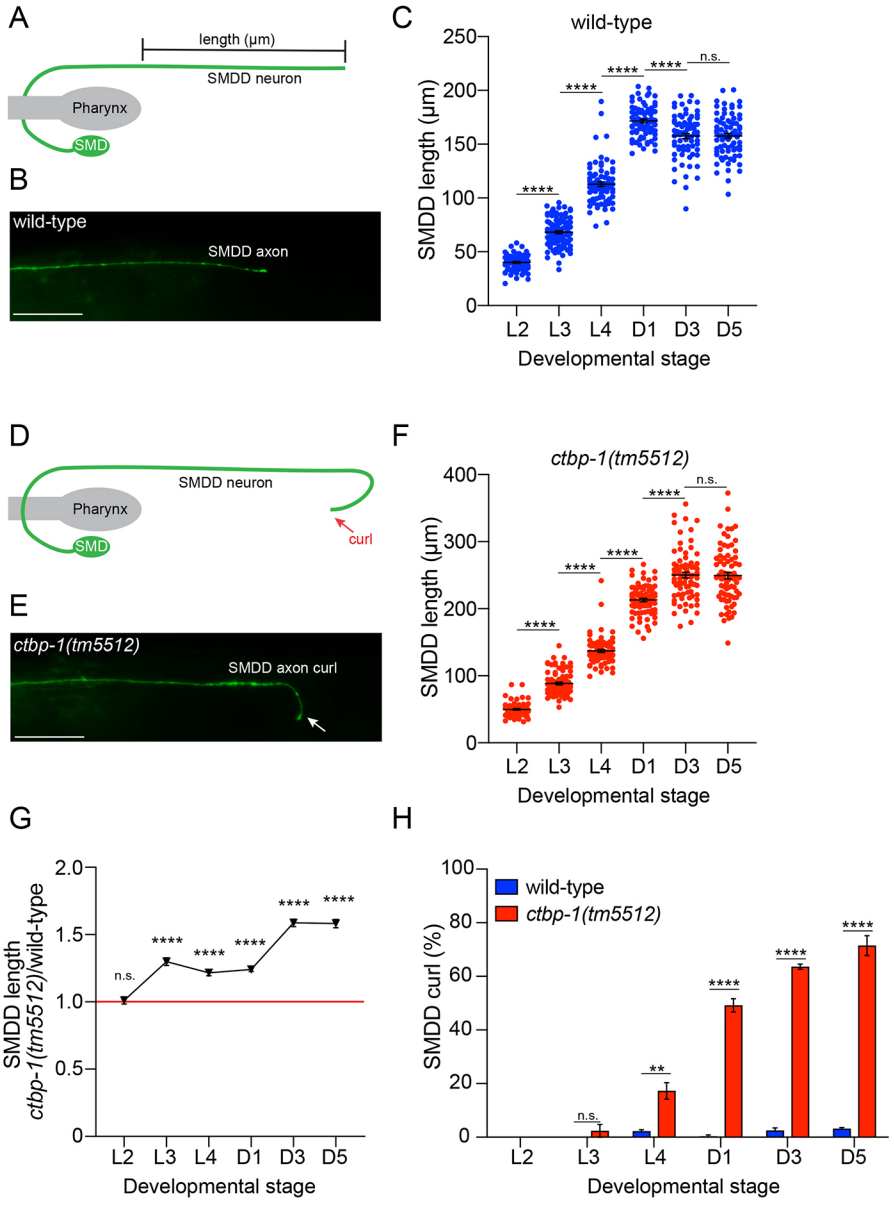

Fig. 1. CTBP-1 regulates SMDD outgrowth and retraction. (A) Schematic of SMDD axon morphology in wild-type worms. Bar shows the axon segment measured in C and F. (B) Image of an SMDD axon in a wild-type L4 larva. (C) Quantification of SMDD axon length during wild-type post-embryonic development (larval stages L2-L4; adult stages D1, D3 and D5). Data presented as individual axon lengths (points) with mean±s.e.m. (bar). *n*=75-91 axons. (D) Schematic of SMDD axon 'curl' defect observed in *ctbp-1(tm5512)* mutant worms. (E) Image of SMDD axon in a *ctbp-1(tm5512)* mutant L4 larva. Arrow indicates the axon curling away from the sublateral nerve cord. (F) Quantification of SMDD axon length during *ctbp-1(tm5512)* post-embryonic development (same developmental stages as in C). Data presented as individual axon lengths (points) with mean±s.e.m. (bar). *n*=73-86 axons. (G) Quantification of SMDD axon length of *ctbp-1(tm5512)* animals, relative to wild-type, during post-embryonic development. Data presented as mean ±s.e.m. (bar). *n*=73-86 axons. (H) Quantification of the SMDD axon curl phenotype in wild-type and *ctbp-1(tm5512)* animals during post-embryonic development (same developmental stages as in C). Data presented as mean±s.e.m. (bar) of three biological replicates, *n*>100 axons. SMDD morphology was visualized by a fluorescent reporter, *rhIs4[Pglr-1::GFP]*. ***P*<0.01, *****P*<0.0001, n.s. not significant (unpaired *t*-test). Scale bars: 20 µm.

Development (2020) 147, dev193805. doi:10.1242/dev.193805

axons of *ctbp-1(tm5512)* mutants were longer than in the wild type, irrespective of whether they extended within the sublateral cord or were misguided outside the cord (Fig. S1B). Because the *ctbp-1(tm5512)* mutant SMDD overgrowth phenotype can already be detected in L3 larvae, the curl phenotype, which is only detectable from the L4 stage, might be caused by premature axon outgrowth (Fig. 1G-H).

The *ctbp-1* locus generates two protein isoforms, CTBP-1a and CTBP-1b. The CTBP-1a isoform contains a sequence-specific THAP (Thanatos-associated protein) DNA-binding domain, a PXDLS-binding cleft that potentially coordinates protein-protein interactions, and a nucleotide-binding dehydrogenase-like domain (Fig. 2A) (Nicholas et al., 2008). CTBP-1b lacks the THAP DNA-binding domain and has a specific N-terminal amino acid sequence (Fig. 2A). Our data show that the *ctbp-1(tm5512)* mutant, in which the *ctbp-1a*-specific THAP DNA-binding domain is disrupted, exhibits defective SMDD axonal development (Fig. 1). We explored whether the THAP DNA-binding domain is required for CTBP-1 control of SMDD development by generating a CTBP-1b-specific deletion, *ctbp-1(aus15)*, using CRISPR-Cas9 (Fig. 2A). We found that *ctbp-1b(aus15)* mutant SMDD axons terminated and retracted normally, had wild-type body length and did not exhibit the axon curl phenotype (Fig. 2B; Fig. S1C,E). Furthermore, animals harboring deletions in both isoforms, *ctbp-1a/b(tm5512aus14)*, exhibited the same axon curl phenotype as the *ctbp-1a(tm5512)* mutant. However, we found that the *ctbp-1a/b* double mutant had longer SMDD axons at the L4 stage than the *ctbp-1a* single mutant (Fig. S1D). These data indicate that CTBP-1a plays the major role in controlling SMDD axon guidance and outgrowth, with CTBP-1b playing a minor function in SMDD outgrowth.

CTBP-1a probably acts cell-autonomously to control SMDD development

To examine where *ctbp-1a* is expressed, we generated a transcriptional *gfp* reporter using 5008 bp of the *ctbp-1a* promoter (*Pctbp-1a::GFP)*. We found that the *Pctbp-1a::GFP* transgene was first detectable in the SMDD neurons at the bean stage of embryogenesis (Fig. 2C). In L4 larvae, the *Pctbp-1a::GFP* transgene drove expression in 12 head neurons, including the SMDD and SMDV neurons (Fig. 2D). The presence of SMDV expression prompted us to examine whether CTBP-1a controls axonal development in the ventral SMDs as it does in the dorsal SMDs. Indeed, we found that the SMDV neurons exhibited developmental defects in *ctbp-1a(tm5512)* animals (Fig. S2A,B).

The neuronal expression pattern of *Pctbp-1a::GFP* suggests that CTBP-1a regulates SMDD development autonomously. To examine this, we first performed transgenic rescue experiments showing that driving *ctbp-1a* cDNA with the *ctbp-1a* promoter fully rescued the SMDD axonal curl and length phenotypes of *ctbp-1a(tm5512)* mutant animals (Fig. 2E; Fig. S2C). Rescue was also observed when driving *ctbp-1a* cDNA using the *lad-2* promoter, which drives expression in the SMDs and 14 other neurons (Aurelio et al., 2002) (Fig. S2D). Together, these data suggest that CTBP-1a regulates SMDD development cell-autonomously.

As predicted by our analysis of the *ctbp-1b(aus15)* mutant, we found that driving *ctbp-1b* expression with the *ctbp-1a* promoter did not rescue the SMDD axonal curl phenotype of *ctbp-1a(tm5512)* mutant animals (Fig. 2F). Because CTBP-1b lacks the THAP DNA-binding domain, we examined whether this domain is necessary and sufficient for CTBP-1a regulation of SMDD development. THAP-containing proteins, including CTBP corepressors, are defined by a highly conserved zinc-coordinating cysteine-containing consensus module that is important for sequence-specific DNA binding (Clouaire et al., 2005; Nicholas et al., 2008). We mutated two conserved cysteines within the full-length CTBP-1a (C5A, C10A) to disrupt THAP domain function and found that this abrogated the ability of CTBP-1a to rescue the *ctbp-1a(tm5512)* SMDD axonal length and curl phenotypes (Fig. 2G; Fig. S2C). Next, we exclusively expressed the THAP domain using the *ctbp-1a* promoter in *ctbp-1a(tm5512)* animals and found that the SMDD axonal length and curl phenotypes were partially rescued (Fig. 2H; Fig. S2C). These data support the requirement for the CTBP-1a THAP domain in regulating SMDD development.

CTBP-1a also houses a conserved PXDLS-binding motif, which is important for interactions with CTBP-1-binding proteins (Nardini et al., 2003). We generated an A203E mutation in the PXDLS-binding motif of full-length CTBP-1a, which was previously shown to abrogate interactions with PXDLS-containing binding proteins (Nardini et al., 2003; Nicholas et al., 2008). We found that the A203E mutation had no detectable effect on the rescuing ability of CTBP-1a in the context of SMDD guidance (Fig. S2E). Together, our data suggest that the intrinsic DNA-binding capacity of the CTBP-1a THAP domain, potentially independent of corepressor proteins, is crucial for the function of CTBP-1a in controlling SMDD development.

The L1CAM LAD-2 and CTBP-1a act in parallel to control SMDD development

L1CAMs are crucial regulators of nervous system development and maintenance. A previous study showed that LAD-2, a *C. elegans* L1CAM ortholog, controls axon guidance of the SMD, SDQL/R and PLN sublateral neurons (Wang et al., 2008). Therefore, we examined whether the functions of CTBP-1a and LAD-2 in controlling SMDD development in *C. elegans* are related. Like *ctbp-1a* mutants, *lad-2(tm3056)* animals exhibited abnormal SMD axon trajectories (curl phenotype) (Fig. 3A) (Wang et al., 2008). We therefore asked whether *lad-2* and *ctbp-1a* control SMDD axon guidance through the same genetic pathway. We found that *lad-2(tm3056)* and *ctbp-1a(tm5512)* single mutants exhibited similar penetrance of SMDD curl phenotype at the L4 stage (Fig. 3A), although the *lad-2(tm3056)* curls occurred earlier (L1 stage) than in *ctbp-1a(tm5512)* animals (L4 stage) (Fig. 1H) (Wang et al., 2008). Interestingly, loss of *ctbp-1a* but not *lad-2* caused an increase in the SMDD curl phenotype between the L4 and adult stages, suggesting that they function in separate pathways to control SMDD guidance (Fig. 3A). Confirming this hypothesis, the SMDD curl phenotype was additive in the *lad-2(tm3056); ctbp-1a(tm5512)* double mutant compared with either single mutant (Fig. 3A). SMDD length in *lad-2(tm3056)* null mutant animals was not significantly different from that in the wild type at L4 and day 1 adult stages and the *lad-2(tm3056); ctbp-1a(tm5512)* double mutant SMDD length was no longer than that of the *ctbp-1a(tm5512)* single mutant (Fig. 3B). We also observed no difference in body length between *lad-2(tm3056)* and wild-type animals (Fig. S1E). We hypothesize that LAD-2 probably acts cell autonomously to control SMDD development, as driving *lad-2* expression with either the *lad-2* or *ctbp-1a* promoter fully rescued the *lad-2(tm3056)* SMDD curl phenotype (Fig. S3A). Taken together, our data suggest that CTBP-1a and LAD-2/L1CAM act cell-autonomously but in parallel genetic pathways to control SMDD development.

As mentioned previously, the SMD neurons extend axons adjacent to those of the SDQL/R and PLN neurons within the sublateral cord (Fig. 3C) (White et al., 1986). Because LAD-2/L1CAM also controls SDQL/R and PLN axonal development, we asked whether CTBP-1a exhibits functional overlap in these

Development (2020) 147, dev193805. doi:10.1242/dev.193805

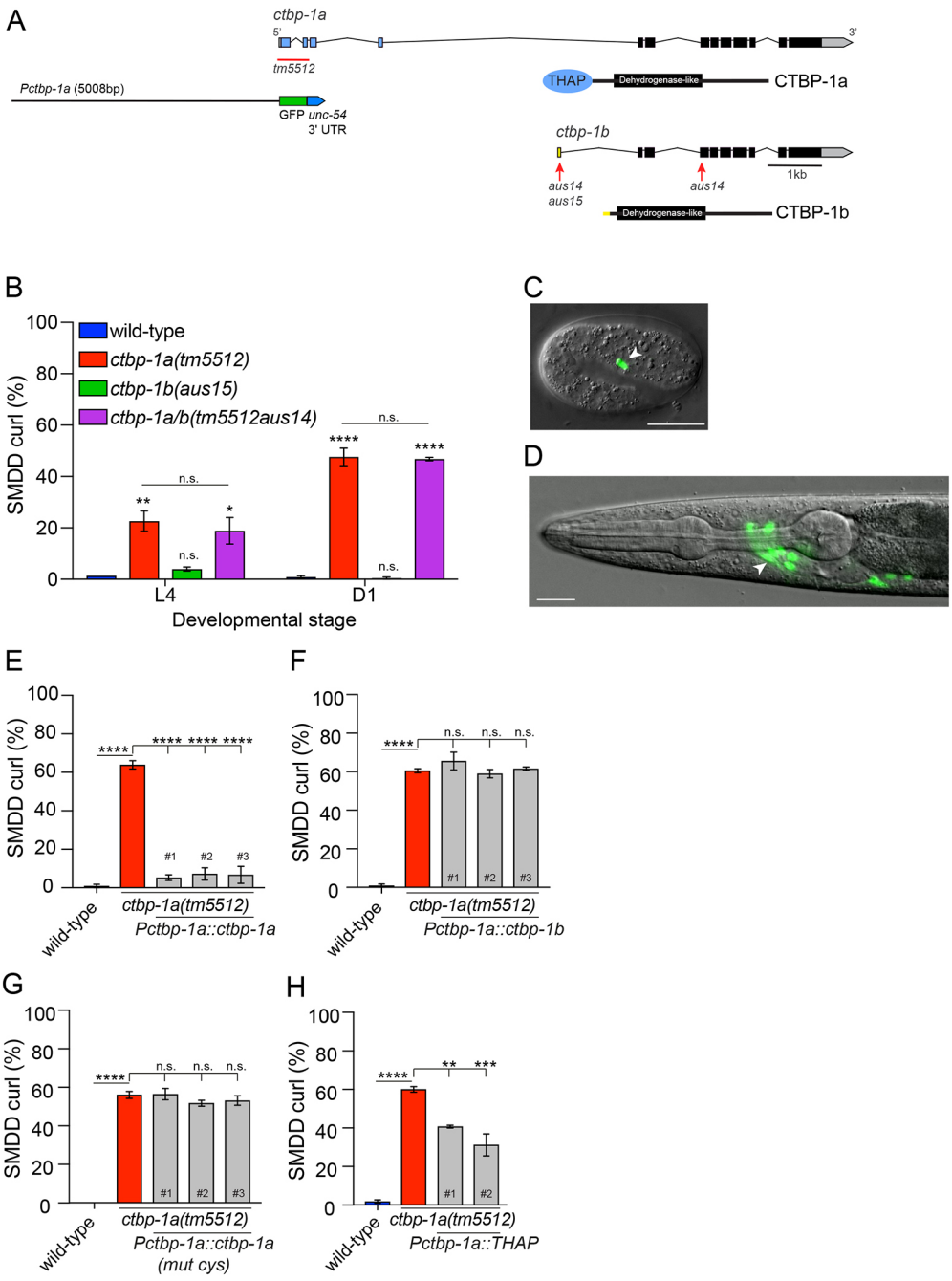

Fig. 2. CTBP-1a probably acts cell-autonomously to control SMDD development. (A) Gene structures and protein domains of *ctbp-1a* and *ctbp-1b*. Shared regions are indicated in black, *ctbp-1a*-specific regions in blue and *ctbp-1b*-specific regions in yellow. Genetic lesions used in this study are indicated by the red bar and arrows. The 5008 bp promoter used for *ctbp-1a* expression analysis is shown by a black line. (B) Quantification of the SMDD axon curl phenotype in wild-type and *ctbp-1* mutants at larval stage 4 (L4) and adult day 1 (D1). (C,D) Expression of a *Pctbp-1a::GFP* transcriptional reporter at the bean stage of embryogenesis (C) and L4 larval stage (D). Nomarski and fluorescence images are overlaid. Arrowheads indicate SMDD neurons. (E) Quantification of SMDD axon curl phenotype of *ctbp-1a(tm5512)* rescue: *ctbp-1a* cDNA under the *ctbp-1a* promoter (5008 bp) rescues the *ctbp-1a(tm5512)* SMDD curl phenotype of day 2 adults (three independent transgenic rescue lines in grey). Data presented as mean±s.e.m. (bar) of three biological replicates, *n*>80 axons. (F) Quantification of SMDD axon curl phenotype of *ctbp-1a(tm5512)* rescue: *ctbp-1b* cDNA under the *ctbp-1a* promoter does not rescue the *ctbp-1a(tm5512)* SMDD curl phenotype of day 2 adults (three independent transgenic rescue lines in grey). (G) Quantification of SMDD axon curl phenotype of *ctbp-1a(tm5512)* rescue: expression of *ctbp-1a(mut cys)* under the *ctbp-1a* promoter does not rescue the *ctbp-1a(tm5512)* SMDD curl phenotype of day 2 adults (three independent transgenic rescue lines in grey). (H) Quantification of SMDD axon curl phenotype of *ctbp-1a(tm5512)* rescue: expression of *ctbp-1a(THAP)* cDNA under the *ctbp-1a* promoter partially rescues the *ctbp-1a(tm5512)* SMDD curl phenotype (two independent transgenic rescue lines in grey). All data are presented as mean±s.e.m. (bar) of three biological replicates, *n*>80 axons. **P*<0.05, ***P*<0.01, ****P*<0.001, *****P*<0.0001, n.s. not significant (one-way ANOVA with Tukey's correction). Scale bars: 20 µm.

neurons (Wang et al., 2008). We found, however, that the SDQL/R and PLN axons developed normally in *ctbp-1a(tm5512)* mutant animals (Fig. 3D,E; Fig. S3B). In addition, deletion of *ctbp-1a* did not enhance the SDQL/R and PLN defects of *lad-2(tm3056)* mutant animals (Fig. 3D,E; Fig. S3B). These data indicate that loss of *ctbp-1a* does not generally disrupt axon guidance within the

Development (2020) 147, dev193805. doi:10.1242/dev.193805

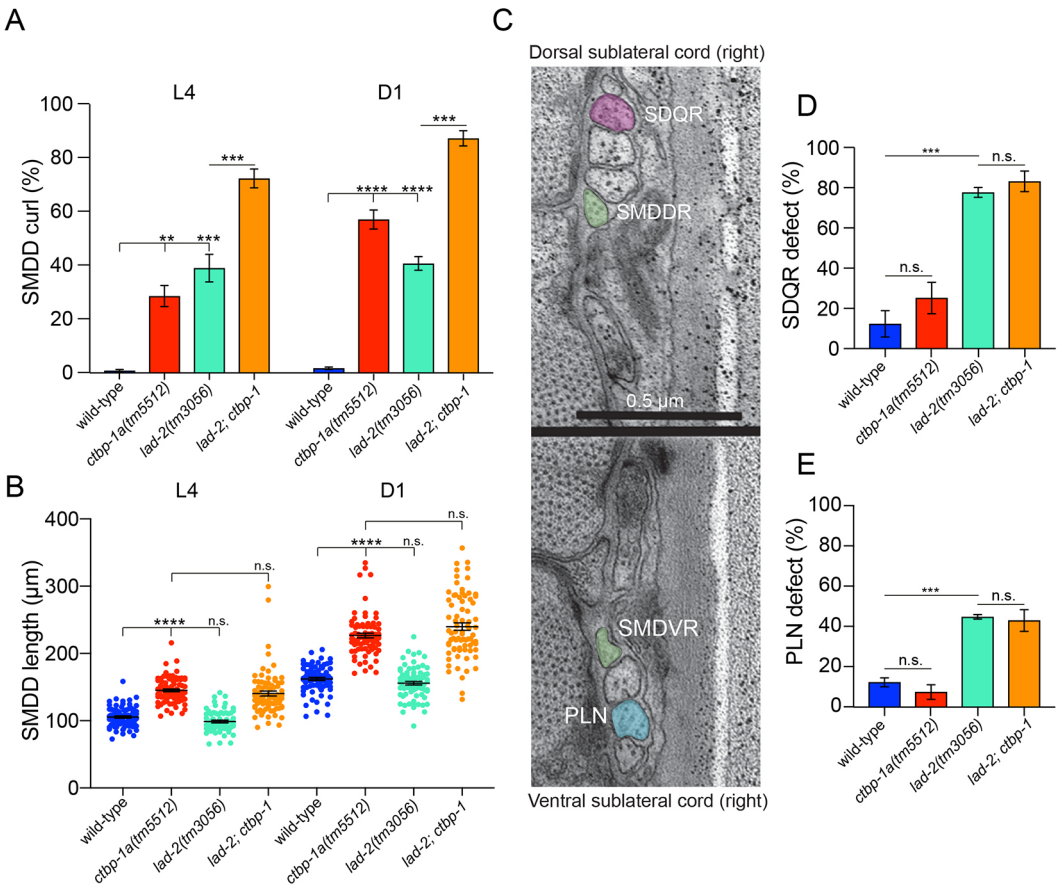

Fig. 3. CTBP-1a acts in a parallel genetic pathway to LAD-2/L1CAM. (A) Quantification of the SMDD curl phenotype of wild-type and mutant animals at larval stage 4 (L4) and adult day 1 (D1). Data presented as mean±s.e.m. (bar) of three biological replicates, *n*>100 axons. (B) Quantification of SMDD length of wild-type and mutant animals at larval stage 4 (L4) and adult day 1 (D1). Data presented as individual axon lengths (points) with mean±s.e.m. (bar). *n*=67-82 axons. (C) SDQR axons (pink) and PLN axons (blue) extend along the right sublateral cords with the SMDD and SMDV axons (green). Transmission electron micrographs of an adult wild-type hermaphrodite provided by David Hall (Albert Einstein College of Medicine, New York, USA). (D,E) Quantification of SDQR (D) and PLN (E) defects of day 1 adults. Data presented as mean±s.e.m. (bar) of three biological replicates, *n*>100 axons. SDQ and PLN morphology was visualized by a fluorescent reporter, *otEx331[Plad-2::GFP]*. ***P*<0.01, ****P*<0.001, *****P*<0.0001, n.s. not significant (one-way ANOVA with Tukey's correction). Scale bar: 0.5 µm.

sublateral cord; instead, it causes defects specifically in the SMDD neurons.

CTBP-1 controls SMDD development by repressing SAX-7/L1CAM expression

Due to the important role of LAD-2/L1CAM in SMDD development, we hypothesized that the other *C. elegans* L1CAM ortholog, SAX-7, also functions in this regard. However, a previous study showed that, unlike LAD-2, SAX-7 is not required for SMD, SDQL/R or PLN development and that loss of *sax-7* does not affect *lad-2* phenotypes in these neurons (Wang et al., 2008). Nevertheless, it is known that inappropriate expression of guidance receptors and their ligands can disrupt neuronal development (Colavita et al., 1998; Hamelin et al., 1993). We therefore hypothesized that CTBP-1, a known transcriptional corepressor, limits SAX-7 expression to enable faithful SMDD development.

The *sax-7* locus encodes long and short protein isoforms that play multiple roles in axonal maintenance and dendritic branching (Fig. 4A) (Bénard et al., 2012; Dong et al., 2013; Pocock et al., 2008; Salzberg et al., 2013; Sasakura et al., 2005). The longer SAX-7 isoform (SAX-7L) contains six Ig-like domains, five FnIII domains and a cytoplasmic tail that houses an ankyrin binding motif, a FERM domain and a PDZ domain (Fig. 4A). The shorter SAX-7 isoform (SAX-7S) lacks the first two Ig-like domains (Fig. 4A). Using the *sax-7(eq1)* allele, which affects both SAX-7 isoforms, we confirmed that SMDD development is not dependent on SAX-7 (Fig. 4A,B). Remarkably, however, loss of *sax-7* partially suppressed the *ctbp-1a(tm5512)* SMDD curl phenotype (Fig. 4B). We confirmed suppression of the *ctbp-1a(tm5512)* SMDD curl phenotype using an independently isolated *sax-7(nj48)* allele, which like *eq1* affects both SAX-7 isoforms (Fig. 4A,B). We next asked whether removal of a specific SAX-7 isoform could suppress the *ctbp-1a(tm5512)* SMDD curl phenotype. To this end, we combined the *ctbp-1a(tm5512)* mutation with either a SAX-7L-specific mutation (*nj53*) or a SAX-7S-specific mutation (*ot820*) (Rahe et al., 2019; Sasakura et al., 2005). We found that removal of SAX-7S but not SAX-7L suppressed the *ctbp-1a(tm5512)* SMDD curl phenotype (Fig. 4B). Furthermore, removal of *sax-7* partially rescued the highly penetrant SMDD curl phenotype of *ctbp-1a(tm5512); lad-2(tm3056)* animals (Fig. S4A). Inappropriate expression of *sax-7s* in the SMDDs caused the *ctbp-1a(tm5512)* mutant phenotype, as low-level expression of *sax-7s*, under the *ctbp-1a* promoter, restored the SMDD curl phenotype to *ctbp-1a(tm5512); sax-7(ot820)* animals (Fig. 4C). However, low-level overexpression of *sax-7s* did not cause the SMDD curl phenotype in wild-type animals (Fig. 4C). This suggests that a threshold of *sax-7s* expression must be reached to cause the SMDD curl phenotype and/or that other CTBP-1 targets are also involved in this axon guidance defect. We next asked whether the increase in SMDD length in *ctbp-*

Development (2020) 147, dev193805. doi:10.1242/dev.193805

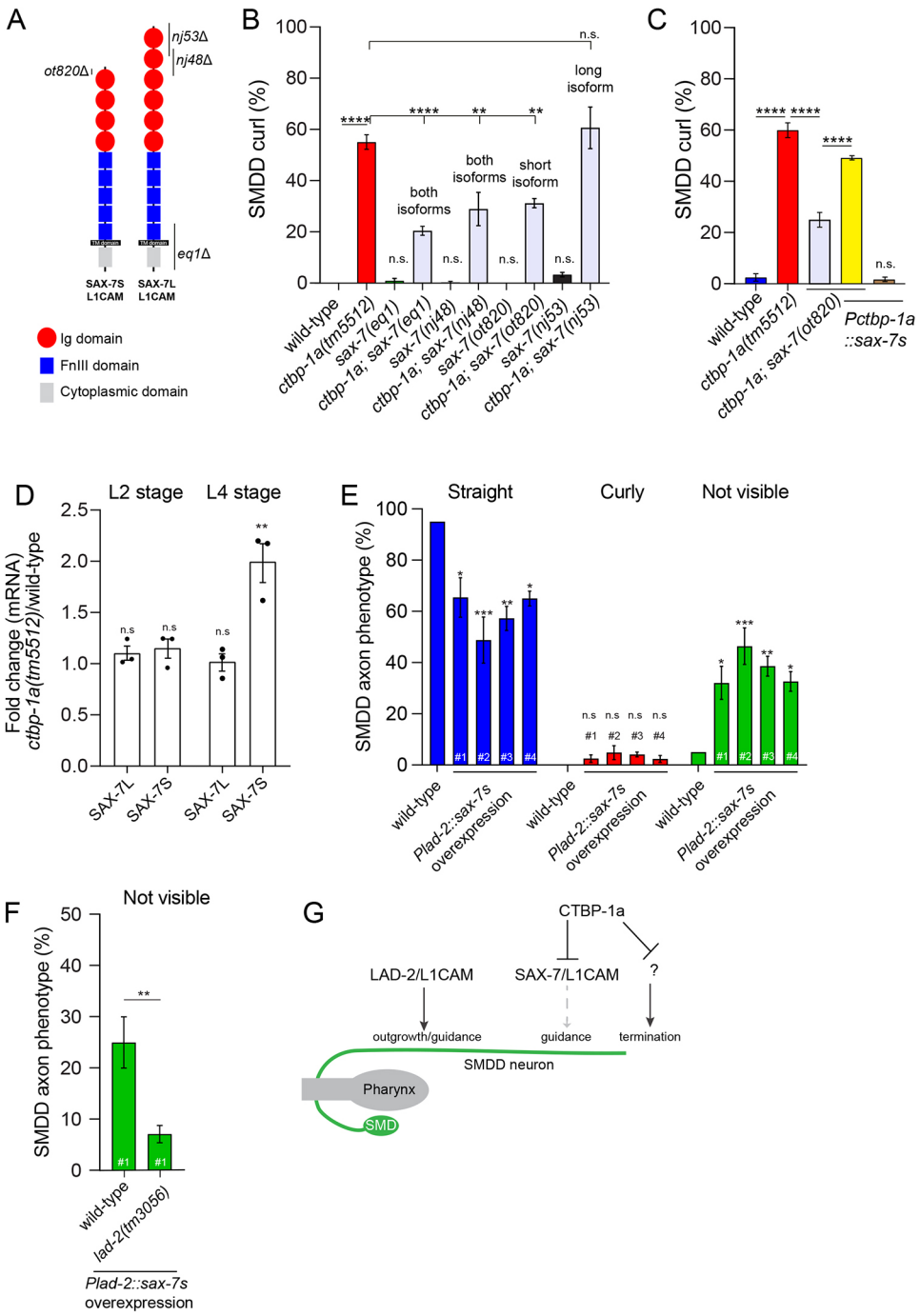

Fig. 4. CTBP-1a regulates *sax-7s* for correct SMDD development. (A) Protein structure of SAX-7S and SAX-7L showing the genetic lesions used in this study (black bars). Ig domain, immunoglobulin domain; FnIII domain, fibronectin domain III; cytoplasmic domain encompasses FERM domain, ankyrin binding domain and PDZ domain. (B) Quantification of the SMDD axon curl phenotype in *sax-7* single and double mutants at adult day 2 (D2). Data presented as mean±s.e.m. (bar) of three biological replicates, *n*>100 axons. ***P*<0.01, *****P*<0.0001, n.s. not significant (one-way ANOVA with Tukey's correction). (C) Quantification of the SMDD axon curl phenotype: low expression of *sax-7* under the *ctbp-1a* promoter (*Pctbp-1a::sax-7s* - 0.2 ng/µl) restores the SMDD curl phenotype to *ctbp-1a(tm5512); sax-7(ot820)* animals. Data presented as mean±s.e.m. (bar) of three biological replicates, *n*>100 axons. *****P*<0.0001, n.s. not significant (one-way ANOVA with Tukey's correction). (D) Expression of *sax-7s* and *sax-7L* transcripts in *ctbp-1a(tm5512)* animals relative to wild-type at the L2 and L4 stages of larval development. qRT-PCR data presented as three biological replicates (points) with mean±s.e.m. (bar). ***P*<0.01, n.s. not significant (one-way ANOVA with Dunnett's multiple comparisons test). (E) Quantification of SMDD axon phenotype of *sax-7s* overexpression in neurons (*Plad-2::sax-7s* - 20 ng/µl, four independent transgenic lines). Data presented as mean±s.e.m. (bar) of three biological replicates, *n*>50 animals. **P*<0.05, ***P*<0.05, ****P*<0.001, n.s. not significant (one-way ANOVA with Dunnett's correction for each phenotype). (F) Quantification of SMDD not visible axon phenotype of wild-type and *lad-2(tm3056)* animals expressing *Plad-2::sax-7s* overexpression line #1. Data presented as mean±s.e.m. (bar) of three biological replicates, *n*>50 animals. ***P*<0.05 (unpaired *t*-test). (G) CTBP-1a represses SAX-7/L1CAM expression to allow correct axon guidance and outgrowth. CTBP-1a regulates SMDD axon termination through an unknown mechanism. In a parallel genetic pathway, LAD-2/L1CAM controls SMDD axon guidance.

1a(tm5512) animals is also dependent on SAX-7S. We found, however, that the *sax-7*(*ot820)* mutation does not affect the length of SMDD axons in wild-type or *ctbp-1a(tm5512)* L4 larvae (Fig. S4B). These data suggest that the molecular mechanisms through which CTBP-1a controls SMDD outgrowth and guidance are distinct.

Our collective genetic data suggest that the *ctbp-1a(tm5512)* mutant SMDD curl phenotype is caused by elevated *sax-7s* (Fig. 4B,C). To examine whether CTBP-1a regulates *sax-7s* expression, we performed quantitative real-time PCR (qRT-PCR) on RNA samples extracted from wild-type and *ctbp-1a(tm5512)* mutant synchronized L2 and L4 larvae (Fig. 4D). Consistent with our phenotypic data, *sax-7s* expression was increased in the *ctbp-1a(tm5512)* mutant compared with wild type in late larval development but not in early larvae (Fig. 4D). In addition, no change in *sax-7L* expression was observed at either larval stage (Fig. 4D). These data suggest that CTBP-1a represses *sax-7s* expression during mid- to late larval stages, directly or indirectly, to enable correct SMDD axon development. If this is the case, one would predict that inappropriate overexpression of SAX-7S in wild-type animals would cause SMDD axon defects. We therefore overexpressed *sax-7s* in wild-type animals and monitored SMDD development. We found that overexpression of *sax-7s* under the *lad-2* promoter caused a severe neomorphic axon outgrowth defect where SMDD axons did not enter the sublateral cord (not visible phenotype), suggesting that the axons did not exit the nerve ring because of defects in axon outgrowth or guidance (Fig. 4E). We

Development (2020) 147, dev193805. doi:10.1242/dev.193805

confirmed that overexpression of *sax-7s* did not cause cell death, as SMDD cell bodies were present in L4 larvae of animals overexpressing *Plad-2::sax-7s* (Fig. S5A). In contrast to overexpression in neurons, overexpression of *sax-7s* in the hypodermis (*dpy-7* promoter) or body wall muscle (*myo-3* promoter), other tissues in which *sax-7* is expressed, had no detectable effect on SMDD development (Fig. S5B,C) (Chen et al., 2001). The neomorphic axon outgrowth phenotype caused by *sax-7s* overexpression in the nervous system was not previously observed in animals lacking *ctbp-1*, *lad-2* or *sax-7*. However, we hypothesized that the axon outgrowth phenotype caused by *sax-7s* overexpression in the SMDD neurons could be a result of inappropriate *in cis* interaction between the two *C. elegans* L1CAMs. To test this hypothesis, we crossed the *lad-2(tm3056)* mutation into one of the *sax-7s* overexpression lines (Fig. 4F). Removing *lad-2* from animals overexpressing *Plad-2::sax-7s* significantly increased the number of SMDD axons entering the sublateral cord (Fig. 4F). These data show that the neomorphic effect caused by *sax-7s* overexpression is dependent on LAD-2. Together, these data reveal that CTBP-1a repression of the short isoform of SAX-7/L1CAM enables LAD-2/L1CAM-driven SMDD axon development.

DISCUSSION

In this study, we found that axons of the *C. elegans* sublateral SMDD motor neurons terminate outgrowth at the first day of adulthood, after which the axons partially retract. Compared with the wild type, animals lacking the CTBP-1 transcriptional corepressor have longer SMDD axons that fail to retract in adults. Loss of CTBP-1 also causes progressive misguidance of SMDD axons outside the sublateral tract. We found that CTBP-1 controls SMDD development by repressing expression of the short isoform of SAX-7/L1CAM. Repression of SAX-7 is crucial for SMDD development, as its overexpression causes severe defects in SMDD outgrowth that are genetically dependent on the other *C. elegans* L1CAM ortholog, LAD-2. Furthermore, we found that LAD-2 acts in a parallel pathway to CTBP-1 and SAX-7/L1CAM to control SMDD development. Hence, elevated LAD-2/L1CAM and reduced SAX-7/L1CAM expression are required to achieve faithful SMDD development (Fig. 4G).

Developmental plasticity of the SMDD axons

Our study reveals that the SMDD axons continuously extend during larval development and into the first day of adulthood. We also found that SMDD axon extension does not directly scale with worm body length, suggesting cell-autonomous control of SMDD length. Why the SMDD axons subsequently retract from day 1 to day 3 of adulthood is unknown. Perhaps the SMDDs perform differential functions in early and late adult life, such that their axons need to be located in distinct environments or they need to modify synaptic connectivity during this period. The ability of the SMDD axons to remodel may also point to a role in experience-dependent learning in response to changing environments. The reported roles for the SMDD neurons in coordinating behavior and circuit function support this hypothesis (Gray et al., 2005; Shen et al., 2016; Yeon et al., 2018).

Parallel regulation of axon development by two L1CAMs

Our work shows that CTBP-1a regulates expression of the short isoform of SAX-7/L1CAM. We found that removal of SAX-7S but not SAX-7L suppresses the SMDD curl phenotype of *ctbp-1a* mutant animals. Correct regulation of SAX-7S expression is crucial, as inappropriate expression of SAX-7S in the SMDDs causes severe axon outgrowth defects such that they do not exit the nerve ring. In contrast, overexpression of SAX-7S in neighboring hypodermis and body wall muscle, which the SMDDs potentially use as a growth substrate (White et al., 1986), has no visible effect on SMDD development. These data suggest that, under standard laboratory conditions, preventing expression of SAX-7S/L1CAM in the SMDDs is required for their development. Our study contrasts with recent findings in *C. elegans* showing that neurite outgrowth depends on SAX-7-mediated fasciculation between adjacent axons (Chen et al., 2019; Ramirez-Suarez et al., 2019). Our results suggest that SAX-7 performs distinct axon outgrowth promoting and inhibiting functions that depend on cellular context.

Our data show that CTBP-1a regulation of SMDD guidance through SAX-7S occurs within a distinct temporal window to LAD-2 (the other *C. elegans* L1CAM). Expression of LAD-2 is detected in the SMDD neurons from birth (Packer et al., 2019; Wang et al., 2008). In congruence, SMDD axon guidance defects caused by loss of LAD-2/L1CAM appear in early L1 larvae (Wang et al., 2008). In contrast, the effects of CTBP-1a loss are not detected until the L4 stage. This suggests that correct development of the SMDD neurons requires precise control of both *C. elegans* L1CAMs over different time scales. This hypothesis is further supported by our experimental evidence: (1) Inappropriately driving *sax-7s* expression with the *lad-2* promoter caused severe SMDD outgrowth defects. (2) SMDD axon defects caused by *sax-7s* overexpression were dependent on *lad-2*. These data suggest that expression of SAX-7S and LAD-2 within the same neuron causes inappropriate adhesion and/or signaling that severely affects axon outgrowth. Could CTBP-1a repression of SAX-7S in the SMDD neurons also provide functional and/or structural flexibility? Perhaps under certain environmental or stress states expression of SAX-7S could be advantageous by providing post-developmental structural integrity to the SMDD neurons or by stimulating axon retraction. For such a scenario, reduction of CTBP-1a levels would promote expression of SAX-7S in the SMDDs. Indeed, CtBP in mice undergoes proteasome-dependent degradation under stress, which may provide alternative strategies for neuronal survival or signaling (Zhang et al., 2003).

Regulation of L1CAMs by THAP-containing proteins is potentially conserved

The CTBP-1a protein contains an N-terminal THAP domain that is defined by a C2CH zinc-dependent DNA-binding motif. THAP domain-containing proteins can act as transcriptional repressors or corepressors either by directly binding to DNA through the C2CH motif or by recruiting corepressor proteins (Clouaire et al., 2005). Our rescue experiments show that mutation of cysteine residues in the C2CH THAP motif of CTBP-1a inhibits its ability to rescue *ctbp-1a(tm5512)* SMDD axonal curl and length phenotypes. Because mutation of the C2CH motif abrogates the DNA-binding activity of THAP proteins, this observation suggests that CTBP-1a can directly regulate transcription (Clouaire et al., 2005). Importantly, these cysteine mutations do not detectably cause THAP1 protein instability (Clouaire et al., 2005). We also found that expression of the CTBP-1a THAP domain is alone sufficient to partially rescue the SMDD axonal curl and length phenotypes of *ctbp-1a(tm5512)* animals. Cumulatively, these data suggest that the THAP domain of CTBP-1a can directly coordinate transcriptional repression and potentially directly repress gene expression in the SMDDs.

Development (2020) 147, dev193805. doi:10.1242/dev.193805

Studies in mammalian models imply that the function of THAP domains in controlling nervous system development and regulation of L1CAM-related molecules may be conserved. Mutations in the *THAP1* gene are associated with dystonia, a brain disorder characterized by involuntary muscle contraction (Zakirova et al., 2018). Additionally, mammalian models of THAP1 loss of function reveal defects in motor function and anxiety-related behavior (Frederick et al., 2019; Ruiz et al., 2015). In these genetic models, *THAP1* heterozygosity can cause a decrease in neuron number within the dentate nucleus of the cerebellum (Ruiz et al., 2015). Additionally, *in vitro* analysis of *THAP1* heterozygous striatal neurons show that neurite growth is defective (Zakirova et al., 2018). These data suggest a common function for THAP proteins in the control of nervous system development and behavior. Additional genomic analysis shows that the regulatory mechanism we elucidated in *C. elegans* may also be conserved in mammals. Differential gene expression analysis of multiple mouse models reveals that heterozygous loss of THAP1 causes dysregulation of L1CAM and related cell adhesion molecules, including NCAM (Aguilo et al., 2017; Frederick et al., 2019). These transcriptomic data need to be validated. However, ChIP-sequencing data (ModENCODE) also show that THAP1 interacts with the L1CAM locus and may therefore directly regulate expression of this SAX-7 ortholog in mammals (C. elegans Sequencing Consortium, 1998; Davis et al., 2018).

Collectively, our results reveal that the CTBP-1a transcriptional corepressor is required for axonal extension of SMDD neurons. Instead of terminating their outgrowth as animals reach adulthood, *ctbp-1a* mutant SMDD axons continue to extend. In addition to regulating axon outgrowth, CTBP-1a is further required for SMDD guidance within the sublateral nerve cord. We found that CTBP-1a controls SMDD guidance, in part by repressing SAX-7/L1CAM expression. This regulatory relationship is crucial, as inappropriate SAX-7/L1CAM expression causes severe defects in SMDD development that are dependent on the presence of LAD-2/L1CAM. Furthermore, expression of LAD-2/L1CAM is required for the early stages of SMDD development in parallel to the CTBP-1a–SAX-7 regulatory axis. Taken together, our results show that the expression of L1CAM family members is tightly regulated to shape axon outgrowth and guidance decisions, control mechanisms we have shown to be mediated by CTBP-1a, a THAP domain transcriptional corepressor protein.

MATERIALS AND METHODS

Experimental model and subject details

Mutant and transgenic reporter strains

Strains were grown using standard growth conditions on NGM agar at 20°C or 25°C on *Escherichia coli* OP50 (Sulston and Brenner, 1974). Neuroanatomical reporter strains used were *rhIs4 Is[Pglr-1::GFP], rpEx1739 Ex[Pctbp-1a::GFP], otEx331 Ex[Plad-2::GFP]*. Detailed strain information is available in Table S3. Developmental stages of animals used for each experiment are specified in the figure legends.

Transgenic lines

Rescue constructs were injected into *rhIs4; ctbp-1a(tm5512)* or *rhIs4; lad-2(tm3056)* mutant backgrounds at 2 ng/µl with *Punc-122::GFP* (20 ng/µl) as injection marker. Overexpression constructs were injected into *rhIs4* (*Pglr-1::GFP*) background at 5-20 ng/µl with *Punc-122::GFP* (20 ng/µl) as injection marker. The *Pctbp-1a::GFP* expression construct was injected into N2 (wild-type) background at 50 ng/µl with *Pttx-3::dsRed2* (50 ng/µl) as injection marker. Microinjections were performed using standard methods (Mello et al., 1991). Briefly, young adult worms were picked to an agarose pad covered with oil on a glass slide. The immobilized worms were injected using FemtoJet 4× injector (Eppendorf) controlled by InjectMan 4 (Eppendorf). Detailed strain information is available in Table S3.

Methods

Molecular cloning

All cloning and mutagenesis was performed using In-Fusion restriction-free cloning (Takara). Linear PCR products and/or vectors (as detailed below) were fused using restriction-free In-Fusion HD cloning reagents. Plasmid sequences were confirmed using Sanger sequencing.

RJP383 *Pctbp-1a::GFP*

The *Pctbp-1a::GFP* reporter construct was generated by cloning the 5008 bp *ctbp-1a* promoter from worm genomic DNA into the promoter-less GFP pPD95.75 expression vector (linearized by HindIII and XbaI).

RJP414 *Pctbp-1a::sax-7s* cDNA

RJP414 was generated by amplifying the pRP13 *Pdpy-7::sax-7s* vector minus the *dpy-7* promoter sequence and amplifying the 5008 bp *ctbp-1a* promoter from RJP383.

RJP422 *Pctbp-1a::ctbp-1a::mCherry*

First, the RJP420 *ctbp-1a::mCherry* vector was generated by amplifying the pPD95.75 mCherry expression vector and amplifying the 2181 bp *ctbp-1a* cDNA from pAER019 *Pglr-1::ctbp-1a::V5::ctbp-1* 3′ UTR (Reid et al., 2015). RJP422 was then generated by cloning the 5008 bp *ctbp-1a* promoter from RJP383 into the RJP420 vector (linearized by BamHI).

RJP423 *Pctbp-1a::ctbp-1b::mCherry*

First, the RJP421 *ctbp-1b::mCherry* vector was generated by amplifying the pPD95.75 mCherry expression vector and amplifying the 1818 bp *ctbp-1b* cDNA from worm cDNA. RJP422 was then generated by cloning the 5008 bp *ctbp-1a* promoter from RJP383 into RJP421 vector (linearized by BamHI).

RJP424 *Plad-2::ctbp-1a::mCherry*

RJP424 was generated by cloning the 4063 bp *lad-2* promoter from worm genomic DNA into the RJP420 vector (linearized with BamHI).

RJP424 *Pdpy-7::ctbp-1a::mCherry*

RJP424 was generated by cloning the 249 bp *dpy-7* promoter from pTB80 *Pdpy-7::GFP* into the RJP420 vector (linearized by BamHI).

RJP515 *Plad-2::sax-7s*

RJP515 was generated by amplifying the *sax-7s* cDNA sequence from RJP414 and amplifying the *lad-2* promoter from RJP424.

RJP514 *Pctbp-1a::ctbp-1a(A203E)::mCherry*

RJP514 was generated using site-directed mutagenesis to mutate the key alanine residue to glutamic acid in the PXDLS-binding cleft domain in the *Pctbp-1a::ctbp-1a cDNA::mCherry* vector (Nicholas et al., 2008).

RJP426 *Pctbp-1a::ctbp-1a(THAP only)::mCherry*

RJP426 was generated by amplifying the sequence corresponding to the 140 amino acid THAP domain of the *Pctbp-1a::ctbp-1a cDNA::mCherry* vector (minus the *ctbp-1b*-shared sequence).

RJP427 *Pctbp-1a::ctbp-1a(C5A,C10A)::mCherry*

RJP427 was generated using site-directed mutagenesis to mutate key cysteines at positions 5 and 10 to alanine in the CTBP-1a THAP domain in the *Pctbp-1a::ctbp-1a cDNA::mCherry* vector (Clouaire et al., 2005).

RJP540 *Pmyo-3::sax-7s*

RJP540 was generated by amplifying the *myo-3* promoter sequence from pPD95.86-*myo-3* and amplifying the *sax-7s* cDNA from RJP414.

RJP517 *Pctbp-1a::lad-2*

RJP517 was generated by amplifying the *Pctbp-1a::GFP* vector (minus GFP) and *lad-2* cDNA from worm cDNA.

Development (2020) 147, dev193805. doi:10.1242/dev.193805

RJP520 *Plad-2::lad-2*

RJP520 was generated by amplifying the *Pctbp-1a::lad-2 cDNA* vector (minus *Pctbp-1*) and *Plad-2* from worm genomic DNA.

CRISPR-Cas9

Single guide (sg)RNA target sequences were designed and incorporated into a *pU6::klp-12* sgRNA expression vector by PCR as previously described (Norris et al., 2015). Wild-type (N2) animals were injected with a mix consisting of the sgRNA expression vector(s) (125 ng/µl), Cas9 expression vector (*Peft-3::cas9::tbb-2*) (50 ng/µl), pCFJ90 (*Pmyo-2::mCherry::unc-54*) (2.5 ng/µl) and pCFJ104 (*Pmyo-3::mCherry::unc-54*) (5 ng/µl). PCR and Sanger sequencing was performed on mCherry-expressing animals to identify deletions. Genome modifications generated in this study were *aus15*, a 4 bp deletion in *ctbp-1b* exon 1, and *aus14*, which contains two lesions, a 39 bp deletion in *ctbp-1b* exon 1/intron 1 and a 5 bp deletion in *ctbp-1b* exon 4b.

Microscopy

Animals were anesthetized with 0.2% levamisole hydrochloride on 5% agarose pads. Images were obtained with an Axio Imager M2 fluorescence microscope, Axiocam 506 mono camera and Zen software (Zeiss).

Phenotypic analyses

SMDD axon morphology assays

SMD morphology was analyzed using the *rhIs4 Is[Pglr-1::GFP]* or *rpEx1739 Ex[Pctbp-1a::GFP]* reporters using the 40× objective. SMDD curl indicates the percentage of SMDD axons that 'curl' away from or leave the dorsal sublateral path along which the SMDD axons extend. SMDD axonal phenotype measures the percentage of axons exhibiting the three possible phenotypes: 'straight', 'curly' and 'not visible'. Straight SMDD axons extend along the dorsal sublateral cord; curly SMDD axons leave the dorsal sublateral cord; and 'not visible' means that there is no axon visible at any position along the dorsal sublateral cord. For each genotype, the total percentages of straight, curly and not visible phenotypes add up to 100%. For all SMDD assays, three biological replicates were performed, and statistical significance was assessed by Student's *t*-test or one-way ANOVA followed by Tukey's or Dunnett's multiple comparisons tests.

SDQL/R and PLN axon morphology assays

SDQR, SDQL and PLN axon guidance assays were performed as previously described, using *otEx331 Ex[Plad-2::GFP]* (Wang et al., 2008). The SDQR axon was scored as defective if the axon extended ventrally. The SDQL axon was scored as defective if the axon extended ventrally. The PLN axon was scored as defective if the axon extended posteriorly. Three biological replicates were performed, and statistical significance was assessed by a one-way ANOVA followed by Tukey's multiple comparisons tests.

SMDD axon length

SMDD axon length images were obtained with a 40× objective using GFP and DIC channels. SMDD axon length (in micrometers) was quantified in FIJI by tracing from the anterior bulb of the pharynx (DIC images) to the distal tip of the axon (GFP fluorescence images) in DIC and GFP composite images. SMDD axons that curled away from the sublateral cord were measured to the end of the axonal tip. Two biological replicates were performed and the measurements pooled for analysis. Statistical significance was assessed by Student's *t*-test or one-way ANOVA followed by Tukey's multiple comparisons test.

Body length

Body length images were obtained with a 20× objective using the DIC channel. Body length images were taken at specified developmental stages at 20× magnification. Body length (in micrometers) was quantified in FIJI (ImageJ) by tracing along the middle of the animal from the anterior tip of the head to the tail. When an animal length spanned more than one image, overlapping images were taken and joined together in Adobe Photoshop. Two biological replicates were performed and the measurements pooled for analysis. Statistical significance was assessed by Student's *t*-test for each developmental stage.

qRT-PCR assays

Total RNA of L4 stage worms was isolated using the RNAeasy mini kit (Qiagen 74104), according to the manufacturer's instructions. Total cDNA was obtained using oligodT primers and the ImProm-II Reverse Transcription System (A3800) followed by quantitative PCR using SYBR green (ThermoFisher Scientific 4385610) and Light Cycler 480 (Roche). Samples from three biological replicates were run in triplicate. The *C. elegans* reference gene *pmp-3* was used as an internal control. Primer sequences are listed in Table S4.

Quantification and statistical analysis

All experiments were performed in three independent replicates, unless specified. The numbers of animals analyzed for specific experiments are reported in the figures or legends. Statistical analysis was performed in GraphPad Prism 8 using an unpaired Student's *t*-test, or one-way analysis of variance (ANOVA) for comparison followed by Tukey's multiple comparison test or Dunnett's multiple comparison test, where applicable. Values are expressed as mean±s.e.m. Differences with $P<0.05$ were considered significant.

Acknowledgements

We thank members of the Pocock Laboratory for comments on the manuscript. We thank David Hall for extraction and annotation of electron micrographs. Some strains were provided by the Caenorhabditis Genetics Center (University of Minnesota), which is funded by NIH Office of Research Infrastructure Programs (P40 OD010440).

Competing interests

The authors declare no competing or financial interests.

Author contributions

Conceptualization: T.S., H.R.N., R.P.; Methodology: T.S., A.H., H.R.N., R.P.; Validation: T.S., H.R.N., R.P.; Formal analysis: T.S., A.H., H.R.N.; Investigation: T.S., A.H., R.P.; Resources: H.R.N., R.P.; Data curation: T.S., H.R.N., R.P.; Writing - original draft: R.P.; Writing - review & editing: T.S., A.H., H.R.N., R.P.; Visualization: T.S.; Supervision: H.R.N., R.P.; Project administration: H.R.N., R.P.; Funding acquisition: H.R.N., R.P.

Funding

This research was supported by an Australian Government Research Training Program (RTP) Scholarship to T.S. This work was supported by a National Health and Medical Research Council Project Grant (GNT1105374) and a Senior Research Fellowship (GNT1137645) (to R.P.) and by a Veski Innovation Fellowship (VIF23 to R.P.).

Supplementary information

Supplementary information available online at
https://dev.biologists.org/lookup/doi/10.1242/dev.193805.supplemental

References

Aguilo, F., Zakirova, Z., Nolan, K., Wagner, R., Sharma, R., Hogan, M., Wei, C. G., Sun, Y. F., Walsh, M. J., Kelley, K. et al. (2017). THAP1: role in mouse embryonic stem cell survival and differentiation. *Stem Cell Rep.* **9**, 92-107. doi:10.1016/j.stemcr.2017.04.032

Aurelio, O., Hall, D. H. and Hobert, O. (2002). Immunoglobulin-domain proteins required for maintenance of ventral nerve cord organization. *Science* **295**, 686-690. doi:10.1126/science.1066642

Bagri, A., Cheng, H.-J., Yaron, A., Pleasure, S. J. and Tessier-Lavigne, M. (2003). Stereotyped pruning of long hippocampal axon branches triggered by retraction inducers of the semaphorin family. *Cell* **113**, 285-299. doi:10.1016/S0092-8674(03)00267-8

Beck, D. B., Cho, M. T., Millan, F., Yates, C., Hannibal, M., O'Connor, B., Shinawi, M., Connolly, A. M., Waggoner, D., Halbach, S. et al. (2016). A recurrent de novo CTBP1 mutation is associated with developmental delay, hypotonia, ataxia, and tooth enamel defects. *Neurogenetics* **17**, 173-178. doi:10.1007/s10048-016-0482-4

Beck, D. B., Subramanian, T., Vijayalingam, S., Ezekiel, U. R., Donkervoort, S., Yang, M. L., Dubbs, H. A., Ortiz-Gonzalez, X. R., Lakhani, S., Segal, D. et al. (2019). A pathogenic CtBP1 missense mutation causes altered cofactor binding and transcriptional activity. *Neurogenetics* **20**, 129-143. doi:10.1007/s10048-019-00578-1

Bénard, C. Y., Blanchette, C., Recio, J. and Hobert, O. (2012). The secreted immunoglobulin domain proteins ZIG-5 and ZIG-8 cooperate with L1CAM/SAX-7

to maintain nervous system integrity. *PLoS Genet.* **8**, e1002819. doi:10.1371/journal.pgen.1002819

Brümmendorf, T., Kenwrick, S. and Rathjen, F. G. (1998). Neural cell recognition molecule L1: from cell biology to human hereditary brain malformations. *Curr. Opin. Neurobiol.* **8**, 87-97. doi:10.1016/S0959-4388(98)80012-3

C. elegans Sequencing Consortium. (1998). Genome sequence of the nematode C. elegans: a platform for investigating biology. *Science* **282**, 2012-2018. doi:10.1126/science.282.5396.2012

Chen, L., Ong, B. and Bennett, V. (2001). LAD-1, the Caenorhabditis elegans L1CAM homologue, participates in embryonic and gonadal morphogenesis and is a substrate for fibroblast growth factor receptor pathway-dependent phosphotyrosine-based signaling. *J. Cell Biol.* **154**, 841-856. doi:10.1083/jcb.200009004

Chen, C. H., Hsu, H. W., Chang, Y. H. and Pan, C. L. (2019). Adhesive L1CAM-Robo signaling aligns growth cone f-actin dynamics to promote axon-dendrite fasciculation in C. elegans. *Dev. Cell* **48**, 215-228.e215. doi:10.1016/j.devcel.2018.10.028

Clouaire, T., Roussigne, M., Ecochard, V., Mathe, C., Amalric, F. and Girard, J.-P. (2005). The THAP domain of THAP1 is a large C2CH module with zinc-dependent sequence-specific DNA-binding activity. *Proc. Natl. Acad. Sci. USA* **102**, 6907-6912. doi:10.1073/pnas.0406882102

Cohen, N. R., Taylor, J. S. H., Scott, L. B., Guillery, R. W., Soriano, P. and Furley, A. J. W. (1998). Errors in corticospinal axon guidance in mice lacking the neural cell adhesion molecule L1. *Curr. Biol.* **8**, 26-33. doi:10.1016/S0960-9822(98)70017-X

Colavita, A., Krishna, S., Zheng, H., Padgett, R. W. and Culotti, J. G. (1998). Pioneer axon guidance by UNC-129, a C. elegans TGF-β. *Science* **281**, 706-709. doi:10.1126/science.281.5377.706

Cook, S. J., Jarrell, T. A., Brittin, C. A., Wang, Y., Bloniarz, A. E., Yakovlev, M. A., Nguyen, K. C. Q., Tang, L. T.-H., Bayer, E. A., Duerr, J. S. et al. (2019). Whole-animal connectomes of both Caenorhabditis elegans sexes. *Nature* **571**, 63-71. doi:10.1038/s41586-019-1352-7

Davis, C. A., Hitz, B. C., Sloan, C. A., Chan, E. T., Davidson, J. M., Gabdank, I., Hilton, J. A., Jain, K., Baymuradov, U. K., Narayanan, A. K. et al. (2018). The Encyclopedia of DNA elements (ENCODE): data portal update. *Nucleic Acids Res.* **46**, D794-D801. doi:10.1093/nar/gkx1081

Dong, X., Liu, O. W., Howell, A. S. and Shen, K. (2013). An extracellular adhesion molecule complex patterns dendritic branching and morphogenesis. *Cell* **155**, 296-307. doi:10.1016/j.cell.2013.08.059

Frederick, N. M., Shah, P. V., Didonna, A., Langley, M. R., Kanthasamy, A. G. and Opal, P. (2019). Loss of the dystonia gene Thap1 leads to transcriptional deficits that converge on common pathogenic pathways in dystonic syndromes. *Hum. Mol. Genet.* **28**, 1343-1356. doi:10.1093/hmg/ddy433

Gray, J. M., Hill, J. J. and Bargmann, C. I. (2005). A circuit for navigation in Caenorhabditis elegans. *Proc. Natl. Acad. Sci. USA* **102**, 3184-3191. doi:10.1073/pnas.0409009101

Hamelin, M., Zhou, Y., Su, M.-W., Scott, I. M. and Culotti, J. G. (1993). Expression of the Unc-5 guidance receptor in the touch neurons of C-elegans steers their axons dorsally. *Nature* **364**, 327-330. doi:10.1038/364327a0

Hildebrand, J. D. and Soriano, P. (2002). Overlapping and unique roles for C-terminal binding protein 1 (CtBP1) and CtBP2 during mouse development. *Mol. Cell. Biol.* **22**, 5296-5307. doi:10.1128/MCB.22.15.5296-5307.2002

Hutter, H. (2019). Formation of longitudinal axon pathways in Caenorhabditis elegans. *Semin. Cell Dev. Biol.* **85**, 60-70. doi:10.1016/j.semcdb.2017.11.015

Luo, L. and O'Leary, D. D. M. (2005). Axon retraction and degeneration in development and disease. *Annu. Rev. Neurosci.* **28**, 127-156. doi:10.1146/annurev.neuro.28.061604.135632

Mello, C. C., Kramer, J. M., Stinchcomb, D. and Ambros, V. (1991). Efficient gene transfer in C. elegans: extrachromosomal maintenance and integration of transforming sequences. *EMBO J.* **10**, 3959-3970. doi:10.1002/j.1460-2075.1991.tb04966.x

Nagaraj, K., Mualla, R. and Hortsch, M. (2014). The L1 family of cell adhesion molecules: a sickening number of mutations and protein functions. *Adv. Neurobiol.* **8**, 195-229. doi:10.1007/978-1-4614-8090-7_9

Nardini, M., Spano, S., Cericola, C., Pesce, A., Massaro, A., Millo, E., Luini, A., Corda, D. and Bolognesi, M. (2003). CtBP/BARS: a dual-function protein involved in transcription co-repression and Golgi membrane fission. *EMBO J.* **22**, 3122-3130. doi:10.1093/emboj/cdg283

Nicholas, H. R., Lowry, J. A., Wu, T. and Crossley, M. (2008). The Caenorhabditis elegans protein CTBP-1 defines a new group of THAP domain-containing CtBP corepressors. *J. Mol. Biol.* **375**, 1-11. doi:10.1016/j.jmb.2007.10.041

Norris, A. D., Kim, H.-M., Colaiácovo, M. P. and Calarco, J. A. (2015). Efficient genome editing in Caenorhabditis elegans with a toolkit of dual-marker selection cassettes. *Genetics* **201**, 449-458. doi:10.1534/genetics.115.180679

Packer, J. S., Zhu, Q., Huynh, C., Sivaramakrishnan, P., Preston, E., Dueck, H., Stefanik, D., Tan, K., Trapnell, C., Kim, J. et al. (2019). A lineage-resolved molecular atlas of C. elegans embryogenesis at single cell resolution. *Science* **365**, eaax1971. doi:10.1126/science.aax1971

Pocock, R., Bénard, C. Y., Shapiro, L. and Hobert, O. (2008). Functional dissection of the C. elegans cell adhesion molecule SAX-7, a homologue of human L1. *Mol. Cell. Neurosci.* **37**, 56-68. doi:10.1016/j.mcn.2007.08.014

Rahe, D., Carrera, I., Cosmanescu, F. and Hobert, O. (2019). An isoform-specific allele of the *sax-7* locus. *MicroPubl Biol*. doi:10.17912/micropub.biology.000092

Ramirez-Suarez, N. J., Belalcazar, H. M., Salazar, C. J., Beyaz, B., Raja, B., Nguyen, K. C. Q., Celestrin, K., Fredens, J., Faergeman, N. J., Hall, D. H. et al. (2019). Axon-dependent patterning and maintenance of somatosensory dendritic arbors. *Dev. Cell* **48**, 229-244.e224. doi:10.1016/j.devcel.2018.12.015

Rapti, G., Li, C., Shan, A., Lu, Y. and Shaham, S. (2017). Glia initiate brain assembly through noncanonical Chimaerin-Furin axon guidance in C. elegans. *Nat. Neurosci.* **20**, 1350-1360. doi:10.1038/nn.4630

Reid, A., Sherry, T. J., Yücel, D., Llamosas, E. and Nicholas, H. R. (2015). The C-terminal binding protein (CTBP-1) regulates dorsal SMD axonal morphology in Caenorhabditis elegans. *Neuroscience* **311**, 216-230. doi:10.1016/j.neuroscience.2015.10.026

Ruiz, M., Perez-Garcia, G., Ortiz-Virumbrales, M., Méneret, A., Morant, A., Kottwitz, J., Fuchs, T., Bonet, J., Gonzalez-Alegre, P., Hof, P. R. et al. (2015). Abnormalities of motor function, transcription and cerebellar structure in mouse models of THAP1 dystonia. *Hum. Mol. Genet.* **24**, 7159-7170. doi:10.1093/hmg/ddv384

Salzberg, Y., Díaz-Balzac, C. A., Ramirez-Suarez, N. J., Attreed, M., Tecle, E., Desbois, M., Kaprielian, Z. and Bülow, H. E. (2013). Skin-derived cues control arborization of sensory dendrites in Caenorhabditis elegans. *Cell* **155**, 308-320. doi:10.1016/j.cell.2013.08.058

Sasakura, H., Inada, H., Kuhara, A., Fusaoka, E., Takemoto, D., Takeuchi, K. and Mori, I. (2005). Maintenance of neuronal positions in organized ganglia by SAX-7, a Caenorhabditis elegans homologue of L1. *EMBO J.* **24**, 1477-1488. doi:10.1038/sj.emboj.7600621

Shen, Y., Wen, Q., Liu, H., Zhong, C., Qin, Y., Harris, G., Kawano, T., Wu, M., Xu, T., Samuel, A. D. T. et al. (2016). An extrasynaptic GABAergic signal modulates a pattern of forward movement in Caenorhabditis elegans. *eLife* **5**, e14197. doi:10.7554/eLife.14197

Sommerville, E. W., Alston, C. L., Pyle, A., He, L., Falkous, G., Naismith, K., Chinnery, P. F., McFarland, R. and Taylor, R. W. (2017). De novo CTBP1 variant is associated with decreased mitochondrial respiratory chain activities. *Neurol. Genet.* **3**, e187. doi:10.1212/NXG.0000000000000187

Sulston, J. E. and Brenner, S. (1974). The DNA of Caenorhabditis elegans. *Genetics* **77**, 95-104.

Tessier-Lavigne, M. and Goodman, C. S. (1996). The molecular biology of axon guidance. *Science* **274**, 1123-1133. doi:10.1126/science.274.5290.1123

Wang, X., Zhang, W., Cheever, T., Schwarz, V., Opperman, K., Hutter, H., Koepp, D. and Chen, L. (2008). The C. elegans L1CAM homologue LAD-2 functions as a coreceptor in MAB-20/Sema2 mediated axon guidance. *J. Cell Biol.* **180**, 233-246. doi:10.1083/jcb.200704178

White, J. G., Southgate, E., Thomson, J. N. and Brenner, S. (1986). The structure of the nervous system of the nematode Caenorhabditis elegans. *Philos. Trans. R. Soc. Lond. B Biol. Sci.* **314**, 1-340. doi:10.1098/rstb.1986.0056

Xu, N.-J. and Henkemeyer, M. (2009). Ephrin-B3 reverse signaling through Grb4 and cytoskeletal regulators mediates axon pruning. *Nat. Neurosci.* **12**, 268-276. doi:10.1038/nn.2254

Yeon, J., Kim, J., Kim, D.-Y., Kim, H., Kim, J., Du, E. J., Kang, K., Lim, H.-H., Moon, D. and Kim, K. (2018). A sensory-motor neuron type mediates proprioceptive coordination of steering in C. elegans via two TRPC channels. *PLoS Biol.* **16**, e2004929. doi:10.1371/journal.pbio.2004929

Zakirova, Z., Fanutza, T., Bonet, J., Readhead, B., Zhang, W., Yi, Z., Beauvais, G., Zwaka, T. P., Ozelius, L. J., Blitzer, R. D. et al. (2018). Mutations in THAP1/DYT6 reveal that diverse dystonia genes disrupt similar neuronal pathways and functions. *PLoS Genet.* **14**, e1007169. doi:10.1371/journal.pgen.1007169

Zhang, Q., Yoshimatsu, Y., Hildebrand, J., Frisch, S. M. and Goodman, R. H. (2003). Homeodomain interacting protein kinase 2 promotes apoptosis by downregulating the transcriptional corepressor CtBP. *Cell* **115**, 177-186. doi:10.1016/S0092-8674(03)00802-X

SUPPLEMENTARY INFORMATION

SUPPLEMENTARY FIGURES

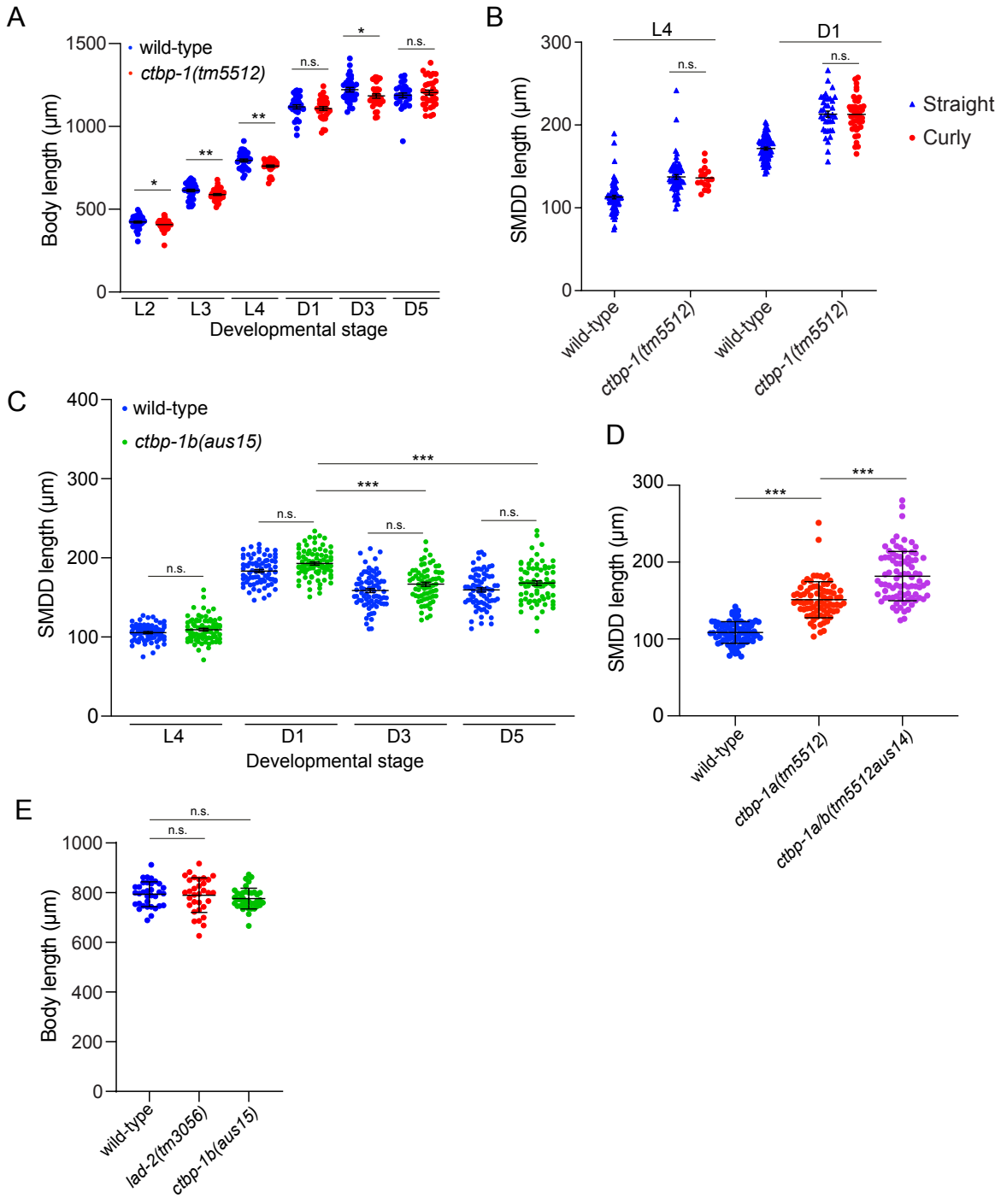

Figure S1. Worm body and SMDD length measurements

(A) Quantification of body length in wild-type and *ctbp-1(tm5512)* animals. Data presented as mean ± S.E.M (bar) of 2 biological replicates, n = 29-42 animals for each developmental stage. *p<0.05, **p<0.01, n.s. - not significant (student's t-test).

(B) Quantification of SMDD axon length in wild-type and *ctbp-1a(tm5512)* animals. Straight axons = blue triangles, curly axons = red dots. *ctbp-1a(tm5512)* mutant axons are the same length whether curly or straight. Data presented as individual straight or curly axons with mean ± S.E.M (bar). n=78-80 axons for each developmental stage. n.s. - not significant (student's t-test).

(C) Quantification of SMDD axon length in wild-type and *ctbp-1b(aus15)* animals. Data presented as individual axon lengths (points) presented as mean ± S.E.M (bar) of 2 biological replicates, n = 70-80 axons for each developmental stage. ***p<0.001, n.s. - not significant (student's t-test).

(D) Quantification of SMDD axon length in wild-type, *ctbp-1a(tm5512)* and *ctbp-1a/b(tm5512aus14)* animals. Data presented as individual axon lengths (points) presented as mean ± S.E.M (bar) of 2 biological replicates, n = 70-84 axons. ***p<0.001.

(E) Quantification of body length in wild-type, *lad-2(tm3056)* and *ctbp-1(aus15)* animals at the L4 stage. Data presented as mean ± S.E.M (bar) of 2 biological replicates, n = 29-44. n.s. - not significant (student's t-test).

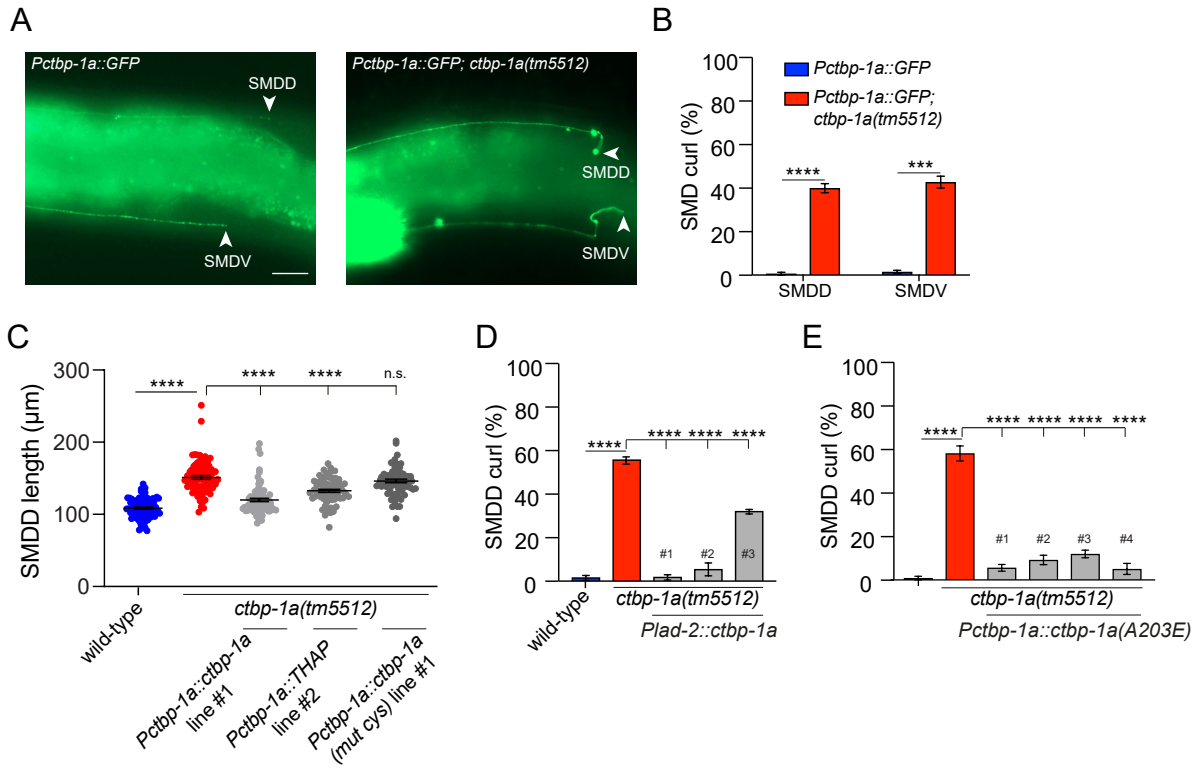

Figure S2. SMDD/V analysis and *ctbp-1a(tm5512)* phenotypic rescue

(A) Expression of the *Pctbp-1a::GFP* transcriptional reporter, showing the SMDD and SMDV axons (arrowheads) in wild-type and *ctbp-1a(tm5512)* mutant animals. Anterior is to the left, ventral is down. Scale bar, 20 µm.

(B) Quantification of SMDD or SMDV curls in wild-type and *ctbp-1a(tm5512)* mutant day 1 adults using the *Pctbp-1a::GFP* reporter. Data presented as mean ± S.E.M (bar) of 3 biological replicates, n>100 axons. ***p<0.001, ****p<0.0001 (unpaired t-test).

(C) Quantification of SMDD axon length of wild-type and *ctbp-1a(tm5512)* rescue animals at the L4 stage: *ctbp-1a* promoter driving *ctbp-1a* cDNA (line #1 from Figure 2E)., THAP domain-only (line #2 from Figure 2H) or *ctbp-1a(mut cys)* (line #1 from Figure 2G). Data presented as individual axon lengths (points) presented as mean ± S.E.M (bar) of 2 biological replicates, n = 70-80. ****p<0.0001, n.s. - not significant (student's t-test).

(D) Quantification of the SMDD axon curl phenotype of *ctbp-1a(tm5512)* rescue: expression of *ctbp-1a* cDNA under the *lad-2* promoter rescues the *ctbp-1a(tm5512)* SMDD curl phenotype of day 2 adults (3 independent transgenic rescue lines in grey). Data presented as mean ± S.E.M (bar) of 3 biological replicates, n> 50 animals. ****p<0.0001 (one-way ANOVA with Tukey's correction).

(E) Quantification of the SMDD axon curl phenotype of *ctbp-1a(tm5512)* rescue: expression of *ctbp-1a(A203A)* cDNA under the *ctbp-1a* promoter rescues the *ctbp-1a(tm5512)* SMDD curl phenotype of day 2 adults (4 independent transgenic rescue lines in grey). Data presented as mean ± S.E.M (bar) of 3 biological replicates, n> 50 animals. ****p<0.0001 (one-way ANOVA with Tukey's correction).

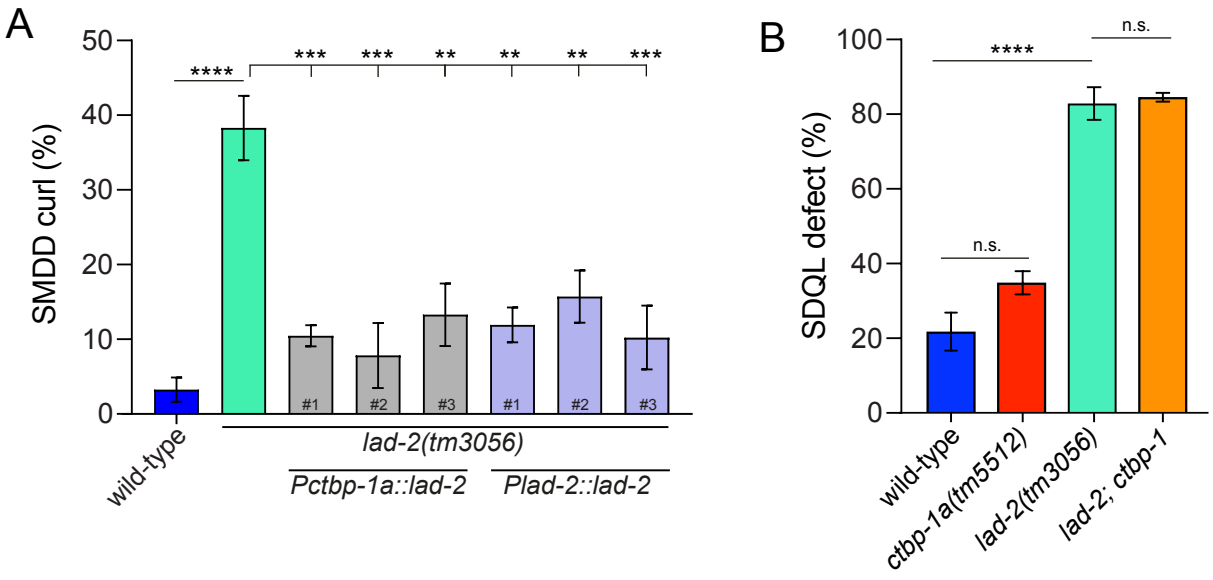

Figure S3. *lad-2* mutant rescue double mutant analysis with *ctbp-1a*

(A) Quantification of SMDD axon curl phenotype of *lad-2(tm3056)* rescue: expression of *lad-2* cDNA under the *lad-2* or *ctbp-1* promoter rescues the *lad-2(tm3056)* SMDD curl phenotype of day 2 adults. (3 independent transgenic rescue lines in grey *Pctbp-1a::lad-2* and blue *Plad-2::lad-2*). Data presented as mean ± S.E.M (bar) of 3 biological replicates, n> 50 animals. **p<0.01, ***p<0.001, ****p<0.0001 (one-way ANOVA with Tukey's correction).

(B) Quantification of the SDQL axon defects in genotypes indicated in day 1 adults. Data presented as mean ± S.E.M (bar) of 3 biological replicates, n> 50 animals. Data presented as mean ****p<0.0001, n.s. - not significant (one-way ANOVA with Tukey's correction).

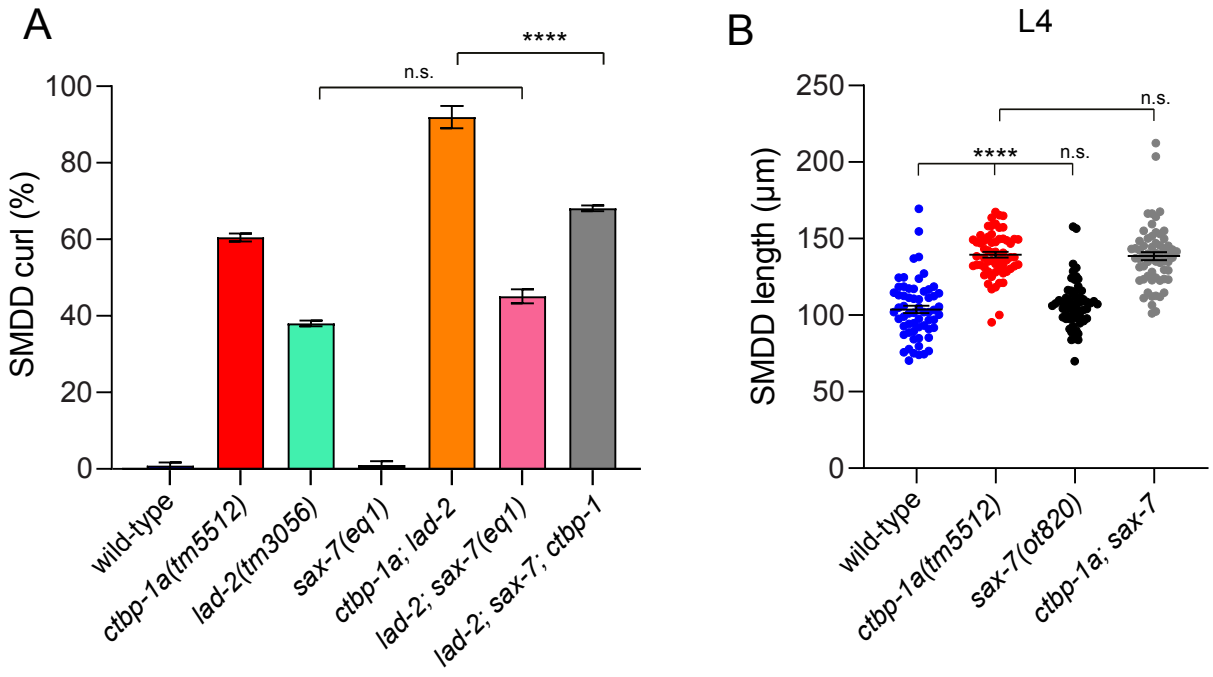

Figure S4. *sax-7* mutant SMDD curl and length analysis

(A) Quantification of SMDD axon curl defect of the triple *sax-7; lad-2; ctbp-1* mutant compared to single and double mutant combinations. ****p<0.0001, n.s. - not significant (one-way ANOVA with Tukey's correction).

(B) Quantification of SMDD axon length in wild-type and *sax-7(ot820)* mutant L4 larvae. Data presented as individual axon lengths (points) with mean ± S.E.M (bar) of 2 biological replicates, n= 59-64 axons for each developmental stage. ****p<0.0001, n.s. - not significant (student's t-test).

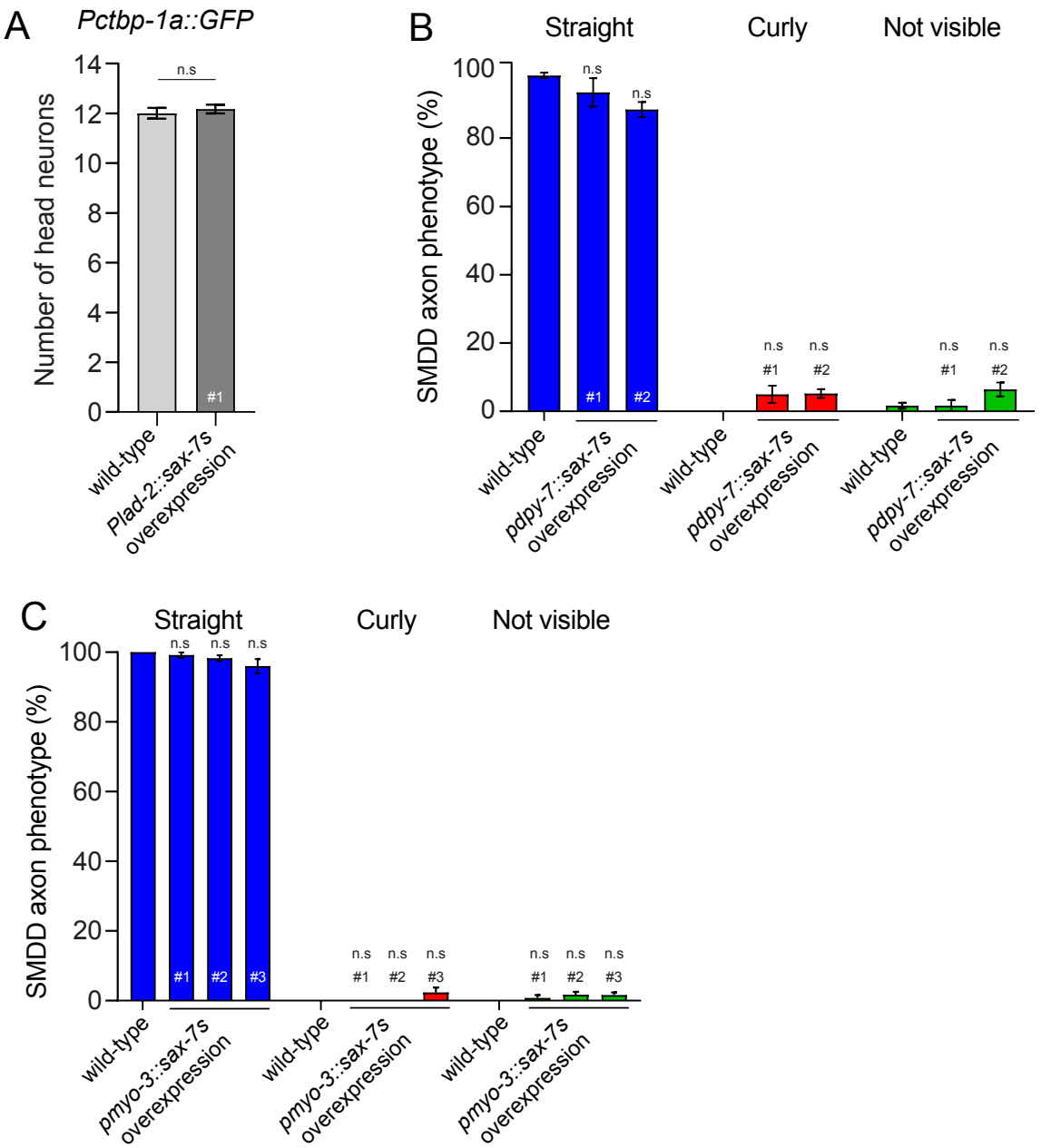

Figure S5. *sax-7s* overexpression analysis

(A) Quantification of *Pctbp-1a::GFP*-expressing head neurons in wild-type L4 larvae +/- the *Plad-2::sax-7s* overexpression transgene (line #1 from Figure 4E-F). Data presented as mean ± S.E.M (bar) of 2 pooled biological replicates, n= 29-34 animals. n.s. - not significant (student's t-test).

(B-C) Quantification of SMDD axon curl phenotype (%) of *sax-7s* overexpression in hypodermis (*Pdpy-7::sax-7s* lines 1-2, B) and muscles (*Pmyo-3::sax-7s* lines 1-3, C). Data presented as mean ± S.E.M (bar) of 3 biological replicates, n>50 animals. n.s. - not significant (one-way ANOVA with Dunnett's correction for each phenotype).

SUPPLEMENTARY TABLES

Table S1. Quantification of body length and SMDD axon length in wild-type animals

Mean body length and SMDD axon length (μm) at larval stages L2-L4 and adult days D1-D5 in wild-type animals. n of animals or axons shown for each developmental stage. Percentage (%) change denotes the change in length from the previous developmental stage (right-hand column).

BODY LENGTH		**n**	**Mean**	**SEM**	**% change**
L2	wild-type	40	422.8	5.7	
L3	wild-type	38	613.1	7.6	145.0
L4	wild-type	34	794.1	8.6	129.5
D1	wild-type	29	1118	13.0	140.8
D3	wild-type	31	1222	13.7	109.3
D5	wild-type	29	1188	14.3	97.2
SMDD AXON LENGTH		**n**	**Mean**	**SEM**	**% change**
L2	wild-type	76	44.54	1.143	
L3	wild-type	91	68.16	1.4	153.0
L4	wild-type	80	112.8	2.1	165.5
D1	wild-type	77	171.7	1.7	152.2
D3	wild-type	75	157.6	2.4	91.8
D5	wild-type	77	157.7	2.2	100.1

Table S2. Quantification of body length

Mean body length and SMDD axon length (μm) at larval stages L2-L4 and adult days D1-D5 in wild-type and *ctbp-1 (tm5512)* mutants. n of animals or axons shown for each developmental stage. Difference between mean of wild-type and *ctbp-1a(tm5512)* at each developmental stage (*ctbp-1(tm5512)*/wild-type) shown (right-hand column).

BODY LENGTH		**n**	**Mean**	**S.E.M**	***ctbp-1(tm5512)*/wild-type**
L2	wild-type	40	422.8	5.7	
	ctbp-1(tm5512)	38	406.6	5.3	96.2
L3	wild-type	38	613.1	7.6	
	ctbp-1(tm5512)	42	588.6	5.2	96.0
L4	wild-type	34	794.1	8.6	
	ctbp-1(tm5512)	33	760.1	7.3	95.7
D1	wild-type	29	1118	13.0	
	ctbp-1(tm5512)	34	1108	11.1	99.1
D3	wild-type	31	1222	13.7	
	ctbp-1(tm5512)	31	1184	12.8	96.9
D5	wild-type	29	1188	14.3	
	ctbp-1(tm5512)	34	1204	14.5	101.3
SMDD AXON LENGTH		**n**	**Mean**	**S.E.M**	***ctbp-1(tm5512)*/wild-type**
L2	wild-type	76	44.54	1.143	
	ctbp-1(tm5512)	73	45.22	1.186	101.5
L3	wild-type	91	68.2	1.4	
	ctbp-1(tm5512)	86	88.5	1.9	129.9
L4	wild-type	80	112.8	2.1	
	ctbp-1(tm5512)	79	137.1	2.3	121.5
D1	wild-type	77	171.7	1.7	
	ctbp-1(tm5512)	80	213.0	2.5	124.1
D3	wild-type	75	157.6	2.4	
	ctbp-1(tm5512)	75	250.1	4.4	158.7
D5	wild-type	77	157.7	2.2	
	ctbp-1(tm5512)	75	249.4	4.9	158.1

Table S3. Strains used in this study

REAGENT or RESOURCE	SOURCE	IDENTIFIER
Wild-type, Bristol strain	CGC	N2
lad-2(tm3056) IV; otEx331[Plad-2::GFP]	Wang et al., 2008	LH247
rhIs4[Pglr-1::GFP] III	This study	HRN169
rhIs4 III; ctbp-1(tm5512) X	This study	HRN226
rhIs4 III; ctbp-1(tm5512aus14) X	This study	HRN551
rhIs4 III; ctbp-1(aus15) X	This study	HRN552
otEx331[Plad-2::GFP]	This study	HRN575
rhIs4 III; lad-2(tm3056) IV; ctbp-1(tm5512) X	This study	HRN585
rhIs4 III; lad-2(tm3056) IV	This study	HRN586
otEx331; lad-2(tm3056) IV; ctbp-1(tm5512) X	This study	HRN587
otEx331; ctbp-1(tm5512) X	This study	HRN588
rhIs4 III; sax-7(nj48) IV	This study	RJP4005
rhIs4 III; sax-7(nj48) IV; ctbp-1(tm5512) X	This study	RJP4006
ctbp-1(tm5512) X	This study	RJP4072
rpEx1739 (Pctbp-1a::GFP + Pttx-3::dsRed2) line 1	This study	RJP4076
rpEx1740 (Pctbp-1a::GFP + Pttx-3::dsRed2) line 2	This study	RJP4077
rpEx1741 (Pctbp-1a::GFP + Pttx-3::dsRed2) line 3	This study	RJP4078
rpEx1742 (Pctbp-1a::GFP + Pttx-3::dsRed2) line 4	This study	RJP4079
rhIs4 III; sax-7(eq1) IV	This study	RJP4080
rhIs4 III; sax-7(eq1) IV; ctbp-1(tm5512) X	This study	RJP4081
rhIs4 III; sax-7(nj53) IV	This study	RJP4082
rhIs4 III; sax-7(nj53) IV; ctbp-1(tm5512) X	This study	RJP4083
ctbp-1(tm5512) X; rpEx1739 (Pctbp-1a::GFP)	This study	RJP4164
rhIs4 III; sax-7(eq1) IV; lad-2(tm3056) IV	This study	RJP4250
rhIs4 III; sax-7(eq1) IV; lad-2(tm3056) IV; ctbp-1(tm5512) X	This study	RJP4251
rhIs4 III; ctbp-1(tm5512) X; rpEx1812 (Pctbp-1a::ctbp-1a::mCherry + Punc-122::GFP) line #1	This study	RJP4270
rhIs4 III; ctbp-1(tm5512) X; rpEx1813 (Pctbp-1a::ctbp-1a::mCherry + Punc-122::GFP) line #2	This study	RJP4271
rhIs4 III; ctbp-1(tm5512) X; rpEx1814 (Pctbp-1a::ctbp-1a::mCherry + Punc-122::GFP) line #3	This study	RJP4272
rhIs4 III; ctbp-1(tm5512) X; rpEx1815 (Pctbp-1a::ctbp-1b::mCherry + Punc-122::GFP) line #1	This study	RJP4278
rhIs4 III; ctbp-1(tm5512) X; rpEx1816 (Pctbp-1a::ctbp-1b::mCherry + Punc-122::GFP) line #2	This study	RJP4279
rhIs4 III; ctbp-1(tm5512) X; rpEx1817 (Pctbp-1a::ctbp-1b::mCherry + Punc-122::GFP) line #3	This study	RJP4280
rhIs4 III; ctbp-1(tm5512) X; rpEx1842 (Pctbp-1a::ctbp-1a THAP only::mCherry + Punc-122::GFP) line #1	This study	RJP4322
rhIs4 III; ctbp-1(tm5512) X; rpEx1843 (Pctbp-1a::ctbp-1a THAP only::mCherry + Punc-122::GFP) line #2	This study	RJP4323
rhIs4 III; rpEx1847 (Pdpy-7::sax-7s + Punc-122::GFP) line #1	This study	RJP4327
rhIs4 III; rpEx1848 (Pdpy-7::sax-7s + Punc-122::GFP) line #2	This study	RJP4328
rhIs4 III; ctbp-1(tm5512) X; rpEx1855 (Pctbp-1a::ctbp-1a (C5A,C10A)::mCherry + Punc-122::GFP) line #1	This study	RJP4339
rhIs4 III; ctbp-1(tm5512) X; rpEx1856 (Pctbp-1a::ctbp-1a (C5A,C10A)::mCherry + Punc-122::GFP) line #2	This study	RJP4340
rhIs4 III; ctbp-1(tm5512) X; rpEx1857 (Pctbp-1a::ctbp-1a (C5A,C10A)::mCherry + Punc-122::GFP) line #3	This study	RJP4341
rhIs4 III; sax-7(ot820) IV; ctbp-1(tm5512) X	This study	RJP4349
rhIs4 III; sax-7(ot820) IV	This study	RJP4360
rhIs4 III; ctbp-1(tm5512) X; rpEx1881 (Pctbp-1a::ctbp-1a (A203E)::mCherry + Punc-122::GFP) line #1	This study	RJP4401
rhIs4 III; ctbp-1(tm5512) X; rpEx1882 (Pctbp-1a::ctbp-1a (A203E)::mCherry + Punc-122::GFP) line #2	This study	RJP4402
rhIs4 III; ctbp-1(tm5512) X; rpEx1883 (Pctbp-1a::ctbp-1a (A203E)::mCherry + Punc-122::GFP) line #3	This study	RJP4403
rhIs4 III; rpEx1891 (Plad-2::sax-7s + Punc-122::GFP) line #1	This study	RJP4418
rhIs4 III; rpEx1892 (Plad-2::sax-7s + Punc-122::GFP) line #2	This study	RJP4419
rhIs4 III; rpEx1893 (Plad-2::sax-7s + Punc-122::GFP) line #3	This study	RJP4420
rhIs4 III; rpEx1894 (Plad-2::sax-7s + Punc-122::GFP) line #4	This study	RJP4421
rhIs4 III; lad-2(tm3056); rpEx1891 (Plad-2::sax-7s + Punc-122::GFP) line #1	This study	RJP4483
rhIs4 III; ctbp-1(tm5512) X; rpEx1874 (Plad-2::ctbp-1a::mCherry + Punc-122::GFP) line #1	This study	RJP4384
rhIs4 III; ctbp-1(tm5512) X; rpEx1875 (Plad-2::ctbp-1a::mCherry + Punc-122::GFP) line #2	This study	RJP4385
rhIs4 III; ctbp-1(tm5512) X; rpEx1876 (Plad-2::ctbp-1a::mCherry + Punc-122::GFP) line #3	This study	RJP4386
rhIs4 III; rpEx2037 (Pctbp-1a::sax-7s) line #1	This study	RJP4573
rhIs4 III; lad-2(tm3056) IV; rpEx2040 (Pctbp-1a::lad-2 + Punc-122::GFP) line #1	This study	RJP4576
rhIs4 III; lad-2(tm3056) IV; rpEx2041 (Pctbp-1a::lad-2 + Punc-122::GFP) line #2	This study	RJP4577
rhIs4 III; lad-2(tm3056) IV; rpEx2042 (Pctbp-1a::lad-2 + Punc-122::GFP) line #3	This study	RJP4578
rhIs4 III; lad-2(tm3056) IV; rpEx2043 (Plad-2::lad-2 + Punc-122::GFP) line #1	This study	RJP4579
rhIs4 III; lad-2(tm3056) IV; rpEx2044 (Plad-2::lad-2 + Punc-122::GFP) line #2	This study	RJP4580
rhIs4 III; lad-2(tm3056) IV; rpEx2045 (Plad-2::lad-2 + Punc-122::GFP) line #3	This study	RJP4581
rpEx1739 (pctbp-1a::GFP); rpEx1891 (plad-2::sax-7s cDNA)	This study	RJP4610
rhIs4 III; sax-7(ot820) IV; ctbp-1(tm5512) X; rpEx2037 (Pctbp-1a::sax-7s) line #1	This study	RJP4611
rhIs4 III; rpEx2073 (Pmyo-3::sax-7s + Punc-122::GFP) line #1	This study	RJP4633
rhIs4 III; rpEx2074 (Pmyo-3::sax-7s + Punc-122::GFP) line #2	This study	RJP4634
rhIs4 III; rpEx2075 (Pmyo-3::sax-7s + Punc-122::GFP) line #3	This study	RJP4635

Table S4. Plasmids used in this study

REAGENT or RESOURCE	SOURCE	IDENTIFIER
Cas9 expression vector (*Peft-3::cas9::tbb-2)*	(Chen et al., 2013)	Addgene plasmid #48960
ctbp-1 sgRNA 1 expression vector 5'-GGTGTTAAATGAAGCTGTGG-3'	This study, modified from (Norris et al., 2015)	N/A
ctbp-1 sgRNA 2 expression vector 5'-GCCAATGGTACTAAACCGACG-3'	This study, modified from (Norris et al., 2015)	N/A
pCFJ90 (*Pmyo-2::mCherry::unc-54)*	(Frokjaer-Jensen et al., 2008)	Addgene plasmid #19327
pCFJ104 (*Pmyo-3::mCherry::unc-54*)	(Frokjaer-Jensen et al., 2008)	Addgene plasmid #19328
Punc-122::GFP (coel::GFP)	(Miyabayashi et al., 1999)	Addgene plasmid #8937
RJP383 *Pctbp-1a::GFP*	This study	RJP383
RJP422 *Pctbp-1a::ctbp-1a::mCherry*	This study	RJP422
RJP423 *Pctbp-1a::ctbp-1b::mCherry*	This study	RJP423
RJP424 *Plad-2::ctbp-1a::mCherry*	This study	RJP424
RJP425 *Pdpy-7::ctbp-1a::mCherry*	This study	RJP425
RJP426 *Pctbp-1a::ctbp-1a(THAP only)::mCherry*	This study	RJP426
RJP514 *Pctbp-1a::ctbp-1a(A203E)::mCherry*	This study	RJP514
RJP427 *Pctbp-1a::ctbp-1a(C5A,C10A)::mCherry*	This study	RJP427
RJP414 *Pctbp-1a::sax-7s cDNA*	This study	RJP414
RJP515 *Plad-2::sax-7s cDNA*	This study	RJP517
RJP540 *Pmyo-3::sax-7s cDNA*	This study	RJP540
pRP13 *Pdpy-7::sax-7s cDNA*	(Pocock et al., 2008)	pRP13
RJP517 *Pctbp-1a::lad-2 cDNA*	This study	RJP517
RJP520 *Plad-2::lad-2 cDNA*	This study	RJP520